Reply to the interactive comments on "Ability of the 4D-Var analysis of the GOSAT BESD XCO$_2$ retrievals to characterize atmospheric CO$_2$ at large and synoptic scales" by Massart et al.

We would like to thank the reviwers for their comments. To reply to the comment of Referee #2 on some missing TCCON data in our study, we downloaded again the TCCON data beginning of November 2015. It appeared that the new downloaded dataset had some additional data for Bremen, Four Corners and Tsukuba and corrected data for Białystok, Karlsruhe and Wollongong (see reply to the interactive comments). We decided to included Bremen and Four Corners in the revised version of the paper. Therefore, Tables 2 and 3 and Figs 2 to 4 had to be modified and the discussion also had to be slightly modified.

Tables 2 has been modified for another reason. In the submitted version of the paper, we used to resample the TCCON data into hourly means. In the new version of the paper, we are using all the available TCCON data as they are.

Some TCCON PIs did not have the chance to participate to the submitted version of the paper. They were offered to participate to the revised version and their name were added in the co-author list. We also updated the author contributions section accordingly.

1   Reply to anonymous Referee #1

1.1   General comments

• *There are, however, some remaining issues regarding the clarity of the manuscript particularly in the description of the different statistics used in the methods section and then ongoing through the paper.*

We changed the description of the different statistics in the new version of

the paper. The bias and the scatter for every individual TCCON station are now described in Eq. 1 with more details. We also added Eq. 2 to define the quantities used in the discussion (model offset, station-to-station bias deviation and model precision). Following a more specific comment of the reviewer, we also included the mean absolute error in Eq. 2 and in the discussion.

● *First, I think it would help to motivate the paper more generally if the authors included a brief description of the key scientific uncertainties relating to the surface emissions and sinks of CO_2. Ultimately, as the authors point out in the conclusions, their work is a stepping stone towards performing source/sink inversion in the future and therefore towards resolving this uncertainties. As it is, the authors only weakly motivate on this subject by saying that monitoring may provide insight into surface fluxes.*

We already replied to this comment in the interactive discussion.

We removed the two sentences starting line 22, page 26275 that were confusing.

We changed the sentence line 26 page 26276 in order to better explain the aim of the study: "The aim of this study is to document the assimilation of XCO_2 products from NIR/SWIR measurements in order to constrain atmospheric CO_2 and to document how the assimilation impacts the simulated atmospheric CO_2 concentration. "

We added the following paragraph in the conclusion: "The variations of the atmospheric reservoir of CO_2 are the result of changes in the surface fluxes to and from the atmosphere. If the quality of the analysis is found to be satisfactory, it could be included into a flux inversion system to infer surface fluxes."

● *Second, the authors have mentioned some of the sources of uncertainties on the GOSAT-BESD XCO_2 retrieval, but this was not done in much detail, nor did the authors discuss what the effects were of these uncertainties on the analysis. The authors explain to readers that filters are already applied during the GOSAT BESD algorithm and also that they include a 2 ppm uncertainty in the observation error covariance matrix for all of the XCO_2 observations used in the assimilation. Can the authors provide any insight into why the value of 2 ppm is chosen? For instance, is this consistent with the typical errors estimated for the XCO_2 retrieval? We are told that observations made under high SZA tend to be removed because these observations are more strongly affected by clouds and aerosols. We are also told that the BESD algorithm explicitly accounts for both clouds and aerosols, when it has to do this, does this lead to higher uncertainties in the retrieval? Are these potential uncertainties fully taken into account with the 2 ppm uncertainty in the error covariance matrix? Can the authors explain what the potential*

effects are of the 2 ppm uncertainty are on the assimilation, and what the effects of unresolved errors might be?

We also replied to this comment in the interactive discussion.

We changed the last paragraph of Sec. 2.1 in the revised version of the paper accordingly to our reply.

• *Finally, do the authors think that the remaining biases in the analysis could be reduced with even more observations and coverage? They have explained that the bias in the analysis likely exists because they do not attempt emission inversion. Is it possible though, that if one had a sufficiently large enough number of observations, could that bias be at least temporarily reduced in the analysis? Do the authors have any plans to try to further reduce the residual bias on the analysis through future work and developments?*

We already replied to this comment in the interactive discussion.

We did not change the text to reply this comment.

1.2 Specific comments

• *Page 26276, line 25. I think it would be worth mentioning that aerosols can also affect the scattering of short wave radiation and therefore can affect the retrieval as well.*

We changed the sentence with: "Sufficiently cloud-free conditions and a low aerosol optical depth are also needed for accurate XCO_2 retrievals."

• *Page 26277, paragraph from line 4 onwards. There are several instances of the use of budget in reference to CO_2 in the atmosphere. Given the context, I am not sure this is the correct technical term to use. Budget refers to the production and loss of something. However, the authors seem to be referring to CO_2 in the atmosphere and how it might change over time. I therefore think something like 'global concentrations' or 'global distribution and abundance' might be more appropriate in this circumstance. Burden might be another option, but this is a single figure referring to the total mass of a gas in the atmosphere.*

We changed part of the paragraph to clarify the text. In particular we replaced those sentences with: "In this model, the production and loss of CO_2 at the surface is based on surface fluxes that are partially prescribed and partially modelled. These CO_2 surface fluxes are not directly constrained by observations and they may deviate from reality. The accumulation of surface fluxes errors then leads to biases in the atmospheric CO_2.."

• *In Section 3.2: I think it would be better if $\hat{c}$ and $\hat{c}^o$ are defined here as well as in the Appendix.*

We changed Section 3.2 in order to better introduce the statistics (see reply to the general comments). The variables $\hat{c}$ and $\hat{c}^o$ are now defined differently: "If $\hat{c}_k^o(t_i)$ for $i \in [1, N_k]$ is the observed TCCON XCO$_2$ time series for the station k and if $\hat{c}_k(t_i)$ for $i \in [1, N_k]$ is the model equivalent time series ...".

We did not change Appendix A as $\hat{c}$ and $\hat{c}^o$ were already defined there. We decided not to introduce the subscript k for the station nor the time in parenthesis in Appendix A in order to keep the appendix simple.

• *It might be better to define bias and scatter in equation 1 with notation rather than with words. Later in the text you refer to bias but use other similar terms, e.g., mean bias. The authors should use notation to remedy this problem.*

See reply to the general comments. We also tried to use the newly introduced notations elsewhere in the discussion.

• *The authors describe the bias as being calculated from the mean, which 'is the simple average'. However, we are not told if this is a temporal or spatial average. Linked to this, if a more formal notation was used in Eq 1., we could see how the average was being calculated.*

See reply to the general comments.

• *Linked to the previous two points, I found that at some points in the paper the authors discussed a bias that is essentially a temporally averaged bias for each station. At other points, the authors use the term mean bias, which is essentially the spatial average of the temporally averaged biases. It would improve the clarity of the discussion if these terms were more distinct from one another and the authors need to do this.*

Using the new notations as suggested by the reviewer, we tried to clarify the text when we used the various terms for the statistics.

• *I found the half paragraph (lines 9 to 16) and the following paragraph (lines 17-23) to be very confusing. Please can the authors try to improve these sections of text. To give some examples: the authors describe 'the sum of', yet Eq 1 does not show any sum; as it stands, the description of offset sounds like bias in Eq 1 - can the authors make these terms more distinct with clearer text and equations; in the second paragraph, it is not clear what is meant by 'each station individually' when compared to descriptions in the previous paragraph.*

This paragraph was removed due to the revision of this section.

- *Please can the authors define offset, station to station bias deviation, and model precision with equations and also include notation for these terms.*

See the reply to the general comments.

- *I would recommend using another statistic: the mean absolute error. Later, when the authors compare the free run and analysis, the mean bias is used to compare both runs. However, the mean bias does not show very clearly that the analysis is greatly improved compared to the free run. The mean bias is still useful, but the mean absolute error shows more substantial improvement in the analysis.*

We would like to thank the reviewer for this recommendation. We introduced the mean absolute error in the paper. First we detailed the definition in Section 3.2 and especially in Eq. 2. Then we used it in Tables 2 and 3 and within the discussion.

- *Page 26279, line 1. I suggest maybe adding 'on cloud and aerosols' prior to '... is mainly ...*

Done.

- *Page 26283, Section 4. I think you can safely remove the first two sentences of Section 4 and begin the third sentence with 'We. . .'.*

Done.

- *Page 26285, lines 12-17. What about the CMDL surface CO_2 measurements in Antarctica? ftp://aftp.cmdl.noaa.gov/data/trace_gases/ These data would make a useful comparison to the free run and analysis over this continent given the lack of satellite observations*

Thank you for the information. In this paper we focused only on the column-average dry-air mole fractions of CO_2 and did not discuss the surface CO_2. For these reason, we do not want to include the surface data.

To be more precise we added "XCO_2" in our sentence: "Unfortunately, there is no independent XCO_2 data available at southern high latitudes to assess the merits of the analysis there."

1.3 Technical comments

We made most of the suggested technical changes. We list hereafter only the changes we made not following exactly the reviewer comment.

- *Page 26276, line 13. Remove 'a' in front of 'four-dimensional'.*

We changed the end of the sentence with: "using a four-dimensional variational (4-D-Var) data assimilation scheme."

- *Page 26283, line 20. I suggest changing 'station-to-station bias variations' to 'the variation of the bias from station to station'.*

We simplified the sentence with: " However, the individual station bias δ_k spans a range from 2.3 ppm at Ascension Island to -2.9 ppm at Białystok."

- *Page 26285, line 1. Insert 'simulated' in between 'of the' and 'atmospheric'.*

Done.

- *Page 26287, line 25. Change '3 times less' to 'more precise'.*

We changed the sentence with: "With a value of 1 ppm, the analysis precision is improved compared to the MACC GOSAT BESD data precision (3.4 ppm for the used version and $\sim$ 2 ppm for the latest version of the product)."

- *Figure 4. Please can you increase the size of the axis labelling.*

We changed the shape of the figure in order to increase its size. We also added the station of Karlsruhe.

- *Figure 7. Please can you increase the size of the axis labelling for latitude and longitude.*

We did not want to increase the size of the axis labelling so to avoid reducing the size of the figures.

2 Reply to anonymous Referee #2

2.1 General comments:

- *In Sect. 2.2 the authors write that they have included in their comparisons all TCCON sites except JPL 2011/Caltech, Dryden, and Eureka, and give good reasons for excluding these sites. However, also Bremen, Ny Ålesund and Tsukuba TCCON sites have been excluded although they were (to my knowledge) operational during year 2013. I would like to know if there is a particular reason for excluding these sites, and if not, I suggest that the authors consider adding them to the revised paper.*

See the reply made for the interactive discussion and the general reply.

- *GOSAT BESD XCO2 retrievals are only one of several independent GOSAT XCO2 retrievals by different teams and retrieval algorithms, and each of these retrievals have their characteristic biases. Even though it is outside the scope of the paper to repeat the assimilation and comparisons for another GOSAT retrieval, I suggest the authors add a brief description and/or*

a literature review about how the GOSAT BESD XCO2 retrievals compare to the other retrievals from GOSAT measurements; at least to the official NIES retrieval product. I think this would be valuable information to the reader because the authors propose that the product of this forecasting system can be considered as an alternative to the satellite XCO2 retrievals.

See the reply made for the interactive discussion where we detailed the characteristics of other GOSAT XCO2 products (from NIES, Leicester and SRON).

We added in the conclusion that: "The precision of the analysis is also better than the documented precision of other GOSAT XCO_2 products. The precision of the NIES product extracted from Yoshida et al.(2013) is 1.8 ppm. The precision of the Leicester and SRON products are respectively 2.5 ppm and 2.37 ppm (Dils et al.,2014)."

• *Are GOSAT BESD XCO2 retrievals not made above the ocean (in the GOSAT glint mode) or were these just excluded in the paper (if so, why)? Some other retrieval algorithms retrieve XCO2 over oceans from the GOSAT glint mode measurements. How would inclusion of ocean retrievals affect the assimilation results?*

See the reply made for the interactive discussion.

No changes were made in the revised version.

2.2 Specific comments:

• *Page 26276, lines 22-23. 'NIR/SWIR measurements based on backscattered solar radiation.' The GOSAT measurements are made from scattered solar radiation, not necessarily backscattered; it depends on the observational geometry.*

We slightly modify the sentence with: "In contrast, column-average dry-air mole fractions of CO_2 (or XCO_2) with a high near-surface sensitivity are retrieved from NIR/SWIR measurements based on scattered or back-scattered solar radiation."

• *Page 26276, line 25. Add 'and a low aerosol optical depth' after 'cloud-free conditions' because aerosols can affect the retrieval quality in addition to clouds.*

Done.

• *Page 26279, lines 13-18. About thinning: was the one data point in $1° \times 1°$ grid cell in target mode retrievals chosen randomly? Why not average all soundings within one grid cell?*

Averaging all the soundings within one grid cell is usually not desired when it comes to the thinning. The assimilation process requires an error associated with the data. The computation of the error on the average value should account for the correlation between the error of the soundings used in the average. As the error correlation is usually not well known, it is difficult to compute an accurate error for the average. Randomly selecting one soundings and the associated error is much simple.

- *Page 26279, lines 24-27. Does 'quality filtering' refer only to SZA filtering, or did you use other criteria in the filtering as well? Please specify.*

The demanding requirements on precision and accuracy of the XCO_2 satellite retrievals require strict quality filtering. In order to minimise bias and scatter of the satellite data, thresholds for selected parameters have been defined. To detail this, we modify the end of the paragraph with: "The reason for this is the filtering of measurements under high solar zenith angle (SZA) conditions where XCO_2 is more challenging to retrieve as the impact of atmospheric scattering becomes larger compared to low SZA conditions. Other data gaps are due to the strict cloud filtering and other filtering like the ones based on the quality of the spectral fits, on scattering parameters, on meteorological state, and on the measurement geometry."

- *Sect. 2.1. Did you apply any bias correction to GOSAT BESD XCO2 data? If so, please add a description of that in the text.*

For the MACC GOSAT BESD XCO_2 dataset, a global offset has been applied. The offset was computed using the TCCON data. As the MACC GOSAT BESD XCO_2 dataset were delivered in near real time and the TCCON data with a delay of few months, it was not possible to create GOSAT and TCCON pairs using a similar geolocation criterion in space and time as for Sect. 4.4 of the paper. Instead the TCCON data from the previous year were used and they were corrected assuming a global atmospheric growth of CO_2. This assumption was reasonable as the mean offset of the MACC GOSAT BESD XCO_2 dataset is 0.04 ppm when compared to the TCCON data of the same year (Table 3). Moreover, as the TCCON data of the same year were not used to correct the global offset of the MACC GOSAT BESD dataset, they remain an independent dataset.

This description was added in the revised version of the paper with the following paragraph: "The MACC GOSAT BESD XCO_2 dataset have been bias corrected using the TCCON data. As this dataset are delivered in near real time and the TCCON data with a delay of few months, it was not possible to directly compare the two data sets. Instead, the TCCON data from the previous year were used and they were corrected assuming a global atmospheric growth of CO_2. A global offset was then computed and applied to the MACC GOSAT BESD XCO_2 based on the comparison between this

dataset and the corrected TCCON dataset of the previous year. Moreover, with this procedure the TCCON data used in this study (same year as for the MACC GOSAT BESD XCO_2 dataset) can be considered as independent data."

• *Sect. 2.1. Did you include both medium and high-gain (M-gain and H-gain) nadir mode GOSAT retrievals in your study? Please specify.*

The MACC GOSAT BESD XCO_2 dataset includes both medium and high-gain nadir mode GOSAT retrievals. We did not filter for a specific gain mode as we did not found any biases between the retrievals of the different gain modes.

We included this information in the revised version: "In brief the algorithm uses three fitting windows, the O_2-A band ($12\,920$–$13\,195\,\mathrm{cm}^{-1}$), a weak CO_2 absorption band (6170–$6278\,\mathrm{cm}^{-1}$) and a strong CO_2 band (4804–$4896\,\mathrm{cm}^{-1}$) from both the medium and high-gain (respectively M-gain and H-gain) GOSAT nadir modes."

• *Sect. 2.2. I think a brief description of the TCCON measurements, instrumentation and accuracy together with references would be appropriate.*

We added few lines and rephrased other of this section in the revised version of the paper: "TCCON is a network of ground-based Fourier Transform Spectrometers recording direct solar spectra in the near infrared spectral region (http://tccon.ornl.gov/). The column-average dry-air mole fractions of CO_2 is retrieved from these spectra together with other chemical components of the atmosphere (Wunch et al., 2011a). In 2014, the version GGG2014 of the TCCON data was released. The errors on the retrieved XCO_2 are documented to be below 0.25% (~ 1 ppm) until the solar zenith angles are larger than $82°$ (http://dx.doi.org/10.14291/tccon.ggg2014.documentation.R0/1221662) When we downloaded the GGG2014 data in November 2015, 20 TCCON stations were reporting data within the time period we are interested in (year 2013)"

• *Page 26283, line 21. The range is even larger: according to Table 2, Ascension has 2.32 ppm. Suggest replacing results for Darwin with the results for Ascension.*

Done

• *Sect. 4.1. The bias in the high Northern latitudes is mostly dictated by the comparison to the Sodankylä TCCON. Adding Ny Ålesund TCCON data might change this dramatically.*

It would be indeed very interesting to see how Ny Ålesund TCCON data would affect the results. These data are not available in the TCCON release we used, even after an update of the TCCON dataset. This is unfortunate

and we could have asked specifically for these data. We did not ask for the data because we wanted to use only the GGG2014 release of the TCCON data so one could carry on a similar study using exactly the same dataset.

- *Page 26287, line 5. I think 'a correction' probably refers to the averaging kernel correction, right? Please specify.*

The correction of the column is not only an averaging kernel correction. We folowed the approach of Dils et al. (2014) where the GOSAT column $\hat{c}_g$ is replaced by $\hat{c}_g'$ before the comptutation of the differnce with the TCCON column. The corrected column $\hat{c}_g'$ uses the GOSAT averaging kernel A_g, the GOSAT a priori profile $\boldsymbol{x}_g^b$ and the TCCON a priori profile $\boldsymbol{x}_t^b$:

$$\hat{c}_g' = \hat{c}_g + \boldsymbol{h}^T \left(A_g - I \right) \left(\boldsymbol{x}_g^b - \boldsymbol{x}_t^b \right) , \tag{1}$$

where $\boldsymbol{h}$ is the vector of the dry-pressure weighted function for all the levels.

We do not think there is a need to add the equation in the revised version as we follow the approach of Dils et al. (2014). Instead, we added the reference in the sentence: "Before computing the difference between each GOSAT/TCCON pair, follwing Dils et al. (2014), we added a correction to the GOSAT retreived value in order to account for the usage of different a priori CO_2 profiles in the two products."

- *Page 26287, lines 6-8. Which TCCON sites were excluded based on this criterion? Please specify in the text.*

Only two stations were excluded by this threshold: Lauder with 27 pairs and Izaña with 12 pairs.

We change the sentence with: " This procedure removes Lauder and Izaña of the list of the used TCCON stations in the comparison and reduces the number stations to 12 (Table 3)."

- *Page 26287, lines 23-28. I find this part difficult to read and follow. Where does the value of 1 ppm refer to? I suggest clarifying these sentences a little.*

We changed this part with: "The analysis has a lower mean absolute error Δ than the one from the MACC GOSAT BESD data (0.65 ppm vs 1. ppm, Table 3), a station-to-station bias deviation σ almost half of the one from GOSAT data (0.7 ppm vs 1.3 ppm) and has an improved precision π (1 ppm vs 3.3 ppm). The mean correlation coefficient is also higher in the analysis than in the satellite data with a value of 0.8 compared to 0.5. The statistics of the MACC GOSAT BESD data found here are different than those of Heymann et al. (2015) who used a more recent version of the product. With the successive improvements in the BESD algorithm, the lastest version has indeed a station-to-station bias deviation of ~ 0.4 ppm and a precision of ~ 2 ppm."

• *Page 26288, lines 4-5. I disagree with the sentence that states that the analysis provides a more accurate and precise representation of the global atmospheric XCO2 field as compared to the satellite data. Based on the results, this is true at the TCCON sites but elsewhere too? We simply do not know.*

We removed this statement in the revised version and the new sentence is: "Moreover, the analysis is able to fill the gaps of the satellite data in time and space."

• *Page 26288, line 18. Should the reference to '(Fig. 7e and b)' be to some other panels (maybe a and b)?*

Thank you, the correct reference is Fig. 7e and f. We changed this in the revised version.

• *Figure 4 in the paper and Supplement, Figs. 1-5. I would suggest adding the co-located GOSAT BESD XCO2 data in the figures as well (in addition to the analysis), using the same geolocation and temporal criteria for the data selection that were mentioned in Sect. 4.4.*

Done.

2.3 Technical corrections:

We made all the suggested technical changes but the ones addressed hereafter.

• *Page 26281, line 3. Change "used to compared a simulation with the TCCON" to "used in comparisons of simulations and the TCCON".*

Done.

• *Page 26285, line 22. I find the word "evident" a little confusing here.*

We changed the sentence with: "Again, the assimilation of the GOSAT data improves the simulated XCO_2 as the free run shows a strong negative bias there."

• *Figure 1 caption. Change "about 3400 data" to "about 3400 data points" or "soundings", "measurements", "retrievals". 1270 similarly. Also please change "GOSAT XCO2" to "GOSAT BESD XCO2".*

We opted for "retrievals".

• *Supplement, Table 1 caption. Change "faction" to "fraction".*

Done.

Ability of the 4-D-Var analysis of the GOSAT BESD XCO$_2$ retrievals to characterize atmospheric CO$_2$ at large and synoptic scales

S. Massart[1], A. Agustí-Panareda[1], J. Heymann[2], M. Buchwitz[2], F. Chevallier[3], M. Reuter[2], M. Hilker[2], J. P. Burrows[2], N. M. Deutscher[2,9], D. G. Feist[4], F. Hase[5], R. Sussmann[6], F. Desmet[7], M. K. Dubey[8], D. W. T. Griffith[9], R. Kivi[10], C. Petri[2], M. Schneider[5], and V. A. Velazco[9]

[1]European Centre for Medium-Range Weather Forecasts, Reading, United Kingdom
[2]Institute of Environmental Physics, University of Bremen, Bremen, Germany
[3]Laboratoire des Sciences du Climat et de l'Environnement, CEA-CNRS-UVSQ, IPSL, Gif sur Yvette, France
[4]Max Planck Institute for Biogeochemistry, Jena, Germany
[5]Karlsruhe Institute of Technology, IMK-ASF, Karlsruhe, Germany
[6]Karlsruhe Institute of Technology, IMK-IFU, Garmisch-Partenkirchen, Germany
[7]University of Antwerp, Antwerp, Belgium
[8]Earth and Environmental Sciences, Los Alamos National Laboratory, Los Alamos, United States
[9]Centre for Atmospheric Chemistry, School of Chemistry, University of Wollongong, Wollongong, Australia
[10]Finnish Meteorological Institute, Arctic Research, Sodankylä, Finland

Correspondence to: S. Massart (sebastien.massart@ecmwf.int)

Abstract. This study presents results from the European Centre for Medium-Range Weather Forecasts (ECMWF) carbon dioxide (CO$_2$) analysis system where the atmospheric CO$_2$ is controlled through the assimilation of ~~column-average~~ column-averaged dry-air mole fractions of CO$_2$ (XCO$_2$) from the Greenhouse gases Observing Satellite (GOSAT). The analysis is compared to a free run simulation (without assimilation of XCO$_2$) and they are both evaluated against XCO$_2$ data from the Total Carbon Column Observing Network (TCCON). We show that the assimilation of the GOSAT XCO$_2$ product from the Bremen Optimal Estimation DOAS (BESD) algorithm during the year 2013 provides XCO$_2$ fields with an improved ~~station-to-station bias deviation of 0.7~~ mean absolute error of 0.6 parts per million (ppm) and an improved station-to-station bias deviation of 0.7 ppm compared to the free run (1.1 ppm and 1.4 ppm, respectively) and an improved estimated precision of ~~∼ 1~~1 ppm compared to the ~~used GOSAT data (3.4~~GOSAT BESD data (3.3 ppm). We also show that the analysis has skill for synoptic situations in the vicinity of frontal systems where the GOSAT retrievals are sparse due to cloud contamination. We finally computed the 10 day forecast from each analysis at 00:00 UTC~~. Compared to its own analysis~~, and we demonstrate that the CO$_2$ forecast shows synoptic skill for the largest scale weather patterns even up to day 5 ~~according to the anomaly correlation coefficient~~compared to its own analysis.

1 Introduction

Carbon in the atmosphere is present mostly in the form of carbon dioxide (CO$_2$). Its amount is relatively small compared to the amount of carbon present in some of the other reservoirs like the ocean (Ciais et al., 2013). Being well mixed, ~~the~~atmospheric CO$_2$ is nevertheless easier to monitor by the ~~mean of in situ measurements than the carbon of some other reservoirs . The atmospheric reservoir varies as a result of changes in the surface fluxes to and from the atmosphere. Monitoring the atmospheric therefore provides insight not only on the atmospheric but potentially provides information about the surface fluxes.~~means of measurements than other reservoirs of carbon. To improve the monitoring of atmospheric CO$_2$, one can combine atmospheric CO$_2$ measurements with a numerical model. This paper describes such a system, which has been developed for the Copernicus Atmosphere Monitoring Service (CAMS).

Rather than using the relatively sparse network of the surface air-sample measurements, here we explore the measurements from satellite sounders in order to have a more global picture of the atmospheric CO_2. To extract information on the CO_2 content in the atmosphere, passive atmospheric remote sounders measure in the thermal infrared (TIR) or in the near infrared / short wave infrared (NIR/SWIR).

The Atmospheric Infrared Sounder (AIRS), measuring in the TIR, detects thermal radiation emitted by the Earth's surface and the atmosphere (Chédin et al., 2003). The assimilation of the AIRS observed radiances was developed by Engelen et al. (2009) at the European Centre for Medium-Range Weather Forecasts (ECMWF) using a four-dimensional variational (4-D-Var) data assimilation scheme. Their results showed the potential of data assimilation to constrain atmospheric CO_2. They also showed the limitations of the assimilation of AIRS radiances, in particular due to the specific vertical sensitivity of the sounder. Due to the low thermal contrast between the Earth's surface and the air masses above, AIRS measurements have limited or no sensitivity to the lower troposphere and higher sensitivity to the middle atmosphere. Because the signals of the CO_2 surface sources and sinks are the largest in the near-surface and lower troposphere, AIRS measurements were not able to capture these signals.

In contrast, column-averaged dry-air mole fractions of CO_2 (or XCO_2) with a high near-surface sensitivity are retrieved from NIR/SWIR measurements based on scattered and back-scattered solar radiation; however, the NIR/SWIR measurements also have their limitations. They need sunlight and are therefore limited to daytime observations. Sufficiently cloud-free conditions and a low aerosol optical depth are also needed for accurate XCO_2 retrievals.

The aim of this study is to document the assimilation of XCO_2 products from NIR/SWIR measurements in order to constrain atmospheric CO_2 and to document how the assimilation impacts the simulated atmospheric CO_2 concentration. For that purpose, we assimilated the XCO_2 products derived from the NIR/SWIR spectra of the Greenhouse gases Observing Satellite (GOSAT, Kuze et. al, 2009). The assimilation system is based on the ECMWF system of Engelen et al. (2009), which has lately evolved for CAMS in order to assimilate retrieved products instead of observed radiances (Massart et al., 2014).

The assimilation system provides an analysis of the atmospheric CO_2 concentration that is then integrated in time using a forecast model. The CO_2 forecast model used in this study is documented by Agustí-Panareda et al. (2014). In this model, the production and loss of CO_2 at the surface is based on surface fluxes that are partially prescribed and partially modelled.

These CO_2 surface fluxes are not directly constrained by observations and they may deviate from reality. The accumulation of surface fluxes errors then leads to biases in the atmospheric CO_2. On the other hand, the strength of the CO_2 forecast model is its ability to provide a realistic CO_2 synoptic variability. The first objective of this study is to determine the quality of the XCO_2 fields resulting from the assimilation of GOSAT XCO_2 data with a CO_2 forecast model where the CO_2 surface fluxes are not constrained.

The atmospheric CO_2 synoptic variability on a regional scale is related to the passage of frontal systems (Wang et al., 2007). These events are difficult to capture with the GOSAT measurements as the availability of the data is limited due to cloud contamination. Therefore, the second objective of this study is to document if the assimilation helps improve the simulation of atmospheric CO_2 for synoptic events despite the lack of measurements nearby.

Within CAMS, ECMWF is providing a CO_2 analysis based on the assimilation of GOSAT XCO_2 data with a delay of 5 days behind real time. A ten day forecast is then issued from the analysis in order to provide the atmospheric CO_2 field in real time and for the next few days. The last objective of this study is to assess the quality of this forecast. The forecast quality as a function of the lead time and the season is evaluated against the analysis.

This paper is structured as follows. Section 2 introduces the data sets used in this study. Section 3 describes our atmospheric CO_2 simulations with and without assimilation of the GOSAT XCO_2 data, and how we compared them with independent measurements. Sections 4 to 6 present the global evaluation of our simulations, a case study and the evaluation of the CO_2 forecast based on the analysis. Finally, Sect. 7 presents our conclusions.

2   Data sets

In this study, we used two sets of data. The first one is the measurements from the GOSAT's Fourier transform spectrometer and the XCO_2 product retrieved from these measurements by the University of Bremen (UoB) and described in Sect. 2.1. The second one is the collection of measurements provided by the Total Carbon Column Observing Network (TCCON) and described in Sect. 2.2.

2.1   GOSAT XCO_2

The GOSAT satellite is a joint effort between the Japanese Aerospace Exploration Agency (JAXA), the National Institute for Environmental Studies (NIES) and the Japanese Ministry of the Environment (MOE) as part of the

Global Change Observation Mission (GCOM) program of Japan. The GOSAT satellite was launched on 23 January 2009 and ~~it~~ carries the Thermal And Near-infrared Sensor for carbon Observations, which consists of a Fourier Transform Spectrometer (TANSO-FTS) and a Cloud and Aerosol Imager (TANSO-CAI).

In this study, we used XCO_2 retrieved from TANSO-FTS measurements of the upwelling radiance at the top of the atmosphere by the Bremen Optimal Estimation DOAS (BESD) algorithm of UoB. The BESD algorithm was initially developed to retrieve XCO_2 from nadir measurements of the SCanning Imaging Absorption spectroMeter for Atmospheric CHartographY (SCIAMACHY) remote sensing spectrometer ~~(Reuter et al., 2010, 2011)~~ on ENVIronment SATellite (ENVISAT, Reuter et al., 2010, 2011). The BESD algorithm has been modified to also retrieve XCO_2 from GOSAT measurements. A detailed description of the GOSAT BESD algorithm can be found in Heymann et al. (2015). In brief, the algorithm uses three fitting windows, the O_2-A band (12 920–13 195 cm^{-1}), a weak CO_2 absorption band (6170–6278 cm^{-1}) and a strong CO_2 band (4804–4896 cm^{-1}) from both the medium and high-gain (respectively M-gain and H-gain) GOSAT nadir modes. An optimal estimation based inversion technique is used to derive the most probable atmospheric state from every individual GOSAT measurement using a priori knowledge. The BESD algorithm explicitly accounts for atmospheric scattering by clouds and aerosols~~which reduces~~, reducing potential systematic biases. The scattering information on cloud and aerosols is mainly obtained from the ~~strong~~ O_2-A and strong CO_2 absorption bands.

We used an inhomogeneous GOSAT BESD XCO_2 dataset in this study as the GOSAT BESD algorithm was still under development. This intermediate version of the GOSAT BESD XCO_2 data is referred to as MACC GOSAT BESD XCO_2 (MACC standing for Monitoring Atmospheric Composition and Climate, the precursor of CAMS). Nevertheless, from beginning of 2014 onwards, we have been assimilating ~~in near real time~~ the current version of the GOSAT BESD data (v01.00.02, Heymann et al., 2015) in near real time.

The TANSO-FTS detector has a circular field of view of 10.5 km when projected on the Earth's surface (at exact nadir). ~~It measured in~~ In 2013~~in~~, it measured in a mode with 3 measurements across track, ~~the footprints being~~ and the footprints were separated by ~ 263 km across track and ~ 283 km along track. The GOSAT satellite ~~could~~ can also operate in target mode resulting in a finer sampling distance. For these specific situations, we further thinned the observations on a $1° \times 1°$ grid by removing all the observations but one. This procedure avoids having several measurements in the same model grid cell during the assimilation. This thinning, plus the characteristics of the instrument (measurement only during sunlit) and the processing of the level-2 data procedure (retrievals for clear-sky conditions and only over land), reduces the number of GOSAT XCO_2 data to about

100 per day. The assimilation window being 12 hours, this means that about 50 GOSAT XCO_2 data ~~are assimilated each time~~ points are assimilated during each time window.

The geographic distribution of these data is very much dependent on the season and the atmospheric conditions as illustrated by Fig. 31. For example, in July 2013 GOSAT BESD data are available up to $75°$ N, in October 2013 they are available only up to $60°$ N. The reason for this is the ~~quality filtering . Measurements~~ solar geometry and the filtering of measurements under high solar zenith angle (SZA) conditions ~~are~~ where XCO_2 is more challenging to ~~evaluate~~ retrieve as the impact of atmospheric scattering becomes larger compared to low SZA conditions. Other data gaps are due to the strict cloud ~~and quality filtering~~ filtering and other filtering like the ones based on the quality of the spectral fits, on scattering parameters, on the meteorological state, and on the measurement geometry.

The MACC GOSAT BESD XCO_2 dataset have been bias corrected using the TCCON data. As this dataset are delivered in near real time and the TCCON data are delivered with a delay of few months, it was not possible to directly compare the two data sets. Instead, the TCCON data from the previous year were used and they were corrected assuming a global atmospheric growth of CO_2. A global offset was then computed and applied to the MACC GOSAT BESD XCO_2 based on the comparison between this dataset and the corrected TCCON dataset of the previous year. Moreover, with this procedure the TCCON data used in this study (same year as for the MACC GOSAT BESD XCO_2 dataset) can be considered as independent data.

For the assimilation, the observation error covariances have to be specified. In this study, we assume that the observation errors are not correlated ~~and the~~ in space and time. For the standard deviation of the observation error, we used the uncertainty of the ~~individual (single ground pixel)~~ BESD XCO_2 ~~retrieval is about~~ product provided together with the data. The BESD XCO_2 uncertainty product accounts for the various sources of uncertainty of the retrieval process. It varies in time and space around an average value of 2 parts per million (ppm). We furthermore established that the specified observation error based on the XCO_2 uncertainty globally matches the expected observation error using diagnostics posterior to the analysis.

2.2 TCCON XCO₂

TCCON is a network of ground-based Fourier Transform Spectrometers recording direct solar spectra in the near infrared spectral region (http://tccon.ornl.gov/). The column-averaged dry-air mole fractions of CO_2 is retrieved from these spectra together with other chemical components of the atmosphere (Wunch et al., 2011a). In 2014, the version GGG2014 of the TCCON data was released. The errors on the retrieved XCO_2 are documented to be below 0.25% (~ 1 ppm) until the solar zenith angles are larger than $82°$

(http://dx.doi.org/10.14291/tccon.ggg2014.documentation.R0/1221662).

When we downloaded the GGG2014 data in November 2015, 20 TCCON stations were providing data within the time period we are interested in (year 2013).

Not all the stations were used in this study. First we removed JPL 2011, Pasadena/Caltech and Tsukuba, as they are not background stations and are associated with significant representativity errors. We also removed Edwards. This station started to retrieve data from the middle of the year 2013, and we assumed that this was not long enough to provide information on the seasonal variation of the error in our simulations. Additionally, we removed Eureka from the list of stations as the site was providing data during only three days in 2013. This selection of the TCCON station made us retain 16 stations (Table 1).

Orléans had a specific treatment compared to the other stations. The averaging kernels were not specified in the GGG2014 release. So we decided to use the same information as for Lamont as advised in the previous release of the TCCON data (version GGG2012).

3   Experimental setup

We ran two model simulations for the year 2013. The first is similar to the operational CAMS CO$_2$ forecast (Agustí-Panareda et al., 2013) and is referred to as the "free run". This simulation is used as the reference to assess the impact of the assimilation of the GOSAT BESD XCO$_2$ data. The second simulation is the analysis in which the GOSAT XCO$_2$ data are assimilated and is referred to as the "analysis". The configuration of both simulations is described in Sect. 3.1. The simulations were evaluated against each other and also against the TCCON data. Section 3.2 introduces the methodology used in comparison of simulations and the TCCON data.

3.1   Model simulations

The global simulations of atmospheric CO$_2$ are performed within the Numerical Weather Prediction (NWP) framework of the Integrated Forecasting System (IFS). The CO$_2$ mass mixing ratio is directly transported within IFS as a tracer and is affected by surface fluxes. The transport is computed online and is updated each 12 h benefiting from the assimilation of all the operational observations within the IFS 4-D-Var assimilation system. The terrestrial biogenic carbon fluxes are also computed online by the carbon module of the land surface model (CTESSEL, Boussetta et al., 2013) while other prescribed fluxes are read from inventories (see Agustí-Panareda et al., 2014 for more details).

The ability to assimilate retrieval products from GOSAT was included in IFS and is detailed in Massart et al. (2014) for the assimilation of methane data. The system used in this study is similar to the one of Massart et al. (2014) and is based on fixed background errors derived from the National Meteorological Center (NMC) method (Parrish and Derber, 1992). The standard deviation of the background error is constant for each model level and slowly increases from the upper troposphere to the lower troposphere with values from about 1 to about 5 ppm, and then rapidly increases to reach a value of about 40 ppm at the surface. The correlation of the background errors varies over the whole domain and vertically with a representative length scale of about 250 km. The system does not account for the spatial or temporal correlation between the errors of the observations.

We chose in this study to have a horizontal resolution of TL255 on a reduced Gaussian grid ($\sim 80\,\text{km} \times 80\,\text{km}$), and 60 vertical levels from the surface up to 0.1 hPa. This resolution is sufficient for resolving the large and synoptic scale horizontal structures of the atmospheric CO$_2$ fields.

3.2   Comparison with TCCON

To evaluate the quality of the model simulations (free run and analysis), we have extensively used the TCCON data in this study. The comparison is performed in the TCCON space using the TCCON a priori and averaging kernel information (see Appendix A for more details). In order to have a decomposition of the errors of the model column-averaged CO$_2$ against the TCCON measurement, we computed for each TCCON station k for $k \in [1, N]$, the mean differences (or bias) δ_k and the standard deviation of differences (or scatter) σ_k over the N_k times t_i for $i \in [1, M_k]$ when we have a TCCON observation for the station k. If $\hat{c}_k^o(t_i)$ for $i \in [1, M_k]$ is the observed TCCON XCO$_2$ time series for the station k and if $\hat{c}_k(t_i)$ for $i \in [1, M_k]$ is the model equivalent time series, then the bias δ_k and scatter σ_k are defined by

$$\delta_k = \frac{1}{M_k} \sum_{i=1}^{M_k} \left[\hat{c}_k(t_i) - \hat{c}_k^o(t_i)\right],$$

$$\sigma_k = \sqrt{\frac{1}{M_k - 1} \sum_{i=1}^{M_k} \left[\hat{c}_k(t_i) - \hat{c}_k^o(t_i) - \delta_k\right]^2}. \qquad (1)$$

Additionally, we computed the correlation coefficient r_k between $\hat{c}_k(t_i)$ and $\hat{c}_k^o(t_i)$ for $i \in [1, M_k]$.

Following Heymann et al. (2015), we also computed the model offset δ, the mean absolute error (MAE) Δ, the station-to-station bias deviation σ and the model precision π for the N TCCON stations

$$\delta = \frac{1}{N}\sum_{k=1}^{N}\delta_k, \qquad \Delta = \frac{1}{N}\sum_{k=1}^{N}|\delta_k|,$$

$$\sigma = \sqrt{\frac{1}{N-1}\sum_{k=1}^{N}[\delta_k - \delta]^2}, \qquad \pi = \frac{1}{N}\sum_{k=1}^{N}\sigma_k. \qquad (2)$$

The statistics for the comparisons of the simulations against the TCCON data have some gaps in time due to availability of the TCCON data. They are also valid only where the TCCON sites are located, i.e. 16 points distributed on the globe. To have a more global overview of the model bias and scatter against the TCCON data, we smoothed these statistics in time and space (see Appendix B for more details). In summary for the bias, we averaged all the model–measurement differences for each TCCON site over a week period. We then fit the time evolution of the weekly bias with a function that combines a linear and a harmonic component for each station. The second step is an extrapolation in space. For each week, the weekly biases of every station are extrapolated using a quadratic function of latitude. This results in a Hovmöller diagram of the bias as a function of time and latitude. A similar process is applied for the scatter (see Figs. 32 and 33).

4 Global evaluation of the analysis

In this section we first present the characteristics of the XCO_2 derived from the free run simulation when compared to the TCCON data. Secondly, we present the impact of the assimilation of the MACC GOSAT BESD XCO_2 comparing the XCO_2 from the analysis against the XCO_2 from the free run. Then, we discuss if the analysis represents an improvement compared to the free run in terms of statistics against the TCCON data. Finally, we discuss the merits of the analysis compared to the MACC GOSAT BESD data once more using the TCCON data as a reference.

4.1 Free run simulation vs. TCCON

When compared with the TCCON data, the free run simulation has a mean offset δ of 0.36 ppm and a mean absolute error Δ of 1.08 ppm (Table 32). However, the individual station bias δ_k spans a range from 2.3 ppm at Ascension Island to −2.9 ppm at Białystok. The station-to-station bias deviation σ of the free run simulation is therefore large with a value of 1.27 ppm.

The variations of the bias as well as the seasonal cycle of the bias are highlighted in the Hovmöller diagram displayed in Fig. 32a. First, it shows that the initial condition of the free run has a positive bias of about 2 ppm over the tropical region when compared to the TCCON data. This bias is reduced during the spring and reappears the next summer. It reaches its highest values in autumn with more than 2 ppm. These results are slightly different from those of Agustí-Panareda et al. (2014) where the model bias was found to be more constant in the tropical region when comparing the background CO_2 in the marine boundary layer with the NOAA GLOBALVIEW-CO2. Here, the evaluation of the bias in the tropics is driven by the comparison with XCO2 measurements from the TCCON station of Ascension Island. For this station, the values of the bias from July to September result from the interpolation process as no measurements were reported during this period (Fig. S1 of the Supplement).

In contrast to the situation at the tropics, the initial condition of the free run has a negative bias at northern mid-latitudes and reaches almost 4 ppm at the latitude of Sodankylä (67° N) when compared to the TCCON XCO_2. This value is the result of the smoothing process as we do not have data for that period (Fig. 34a). The negative bias at these mid-latitudes is nevertheless confirmed by the comparison with other stations, like Karlsruhe and Park Falls, where we have some data at the beginning of the year (Figs. 34b and 34c). The negative bias at mid-latitudes remains high during the whole year, with an absolute value generally greater than 1 ppm and larger at the end of spring, and in June and December. This can be explained by the fact that the model does not release enough CO_2 before and after the growing season, i.e. March to May and October to December, and by the fact that the onset of the CO_2 sink associated with the growing season starts too early in the model (Agustí-Panareda et al., 2014).

The precision π of the free run measured by the average scatter between the simulation and the TCCON data is 1.4 ppm (Table 32). Similarly to the bias, the scatter presents some variation in time and space (Fig. 33a). The Hovmöller diagram highlights the northern mid-latitudes during May–June–July when the scatter has its highest values of more than 1 ppm. This increase in the scatter is driven by the behaviour of the free

run at Sodankylä where the simulation has a lot of variability and the measurements show no variability (Fig. 34a). Elsewhere, there is also an increase of the scatter between May and July which is during the growing season. This increase could be explained by the issues of the model or by higher variability of the simulated atmospheric CO$_2$ during this season.

4.2 Analysis vs. free run

To assess the impact of the assimilation of the MACC GOSAT BESD XCO$_2$, we compared the evolution of XCO$_2$ from the analysis with XCO$_2$ from the free simulation. Figure 35 presents the Hovmöller diagram (time vs. latitude) of the difference. It shows that the first region where the analysis impacts XCO$_2$ is the tropics. There, compared to the free run, the analysis continuously decreases XCO$_2$, up to 1 ppm in June and more than 2 ppm from September to December. The assimilation of the GOSAT data consequently causes an improvement as the free run has a positive bias in this region in autumn compared to the TCCON data.

The analysis also decreases XCO$_2$ over the southern extra tropics when compared to the free run. The decrease extends to the southern high latitudes even when no GOSAT data were assimilated in this region. This decrease results mainly from the transport of CO$_2$ from the equatorial region and mid-latitudes towards high latitudes. Unfortunately, there are no independent XCO$_2$ data available at southern high latitudes to assess the merits of the analysis there.

Despite the fact that some GOSAT data are assimilated in the northern mid-latitudes during the first months of the simulation, the analysis only starts to differ significantly from the free run from March onwards. In this region, north of 30° N, the analysis has higher values of XCO$_2$ than the free run, with a difference of more than 2 ppm during the northern summer. Again, the assimilation of the GOSAT data improves the simulated XCO$_2$ as the free run shows a strong negative bias there. Similar to the behaviour discussed for the southern high latitudes, the change in the CO$_2$ concentration at northern mid-latitudes is transported northward to higher latitudes. There is, nevertheless, a difference between the two hemispheres. For the Northern Hemisphere we have more data at high latitudes, especially during the summer when the northernmost GOSAT measurements cover goes up to 80° N.

4.3 Analysis vs. TCCON data

When compared with the TCCON data, the GOSAT BESD XCO$_2$ analysis has an offset δ of -0.34 ppm and a mean absolute error Δ of 0.57 ppm (Table 32). The offset is similar to that of the free

run (-0.36 ppm), but the mean absolute error is improved (1.08 ppm for the free run). The individual station bias is moreover more constant in time for the analysis compared to the free run. For example, the trend of the free run bias is 2.08 ppm yr^{-1} for Lauder (Table S1 of the Supplement), and it improves to 0.47 ppm yr^{-1} for the analysis (Table S2 of the Supplement and Fig. 34c).

By increasing XCO$_2$ in the northern mid-latitudes as discussed before, the analysis considerably reduces the bias. A residual seasonal cycle in the bias is still present, with values usually in the range of 0 to 3 ppm (Fig. 32b). This could be explained by the fact that we correct the atmospheric state of CO$_2$ and not the CO$_2$ fluxes. During the seasons when the CO$_2$ fluxes are the main driver of the atmospheric CO$_2$, the optimisation of the atmospheric state only may not be enough.

The analysis has a more constant bias in time than the free run. It is also more accurate in space, with a station-to-station bias deviation σ that is largely reduced compared to the free run with a value of 0.61 ppm against 1.27 ppm (Table 32). The assimilation of the MACC GOSAT BESD XCO$_2$ thus helps significantly improve the accuracy of the model. The assimilation also helps improve the precision π, with the mean scatter improved by 15 %, to a value of 1.22 ppm. The scatter of the analysis is reduced for all TCCON stations compared to the free run except for Garmisch where the scatter remains similar. The Hovmöller diagram of the scatter shows that the main reduction is in the northern high latitudes in May (Fig. 33). In particular, the analysis shows less spurious variability than the free run at Sodankylä (Fig. 34a).

4.4 Analysis vs. MACC GOSAT BESD data

The analysis proves to be much more accurate and more precise than the free run when compared to the TCCON data. The analysis also fills the gaps in time and space of the MACC GOSAT BESD data. In this section, we evaluate the analysis against the MACC GOSAT BESD data once more using the TCCON data as a reference.

The MACC GOSAT BESD data were compared to the TCCON data using a geolocation criterion of 5° in space and a time window of ± 2 h. Before computing the difference between each GOSAT/TCCON pair, following Dils et. al (2014), we added a correction to the GOSAT retrieved value in order to account for the usage of different a priori CO$_2$ profiles in the two products. Moreover, we only kept the stations where more than 30 GOSAT/TCCON pairs were found in order to have more robust statistical results. This procedure removes Lauder and

Izaña from the list of the used TCCON stations in the comparison and reduces the number of stations to 12 (Table 3).

For each GOSAT/TCCON pair, we extracted the CO$_2$ profile from the analysis at the same location and time as the GOSAT measurement before computing the difference between the model and the TCCON data. In this way, we have a fair comparison between the analysis and the MACC GOSAT BESD data with respect to the TCCON data.

The resulting subset of the analysis minus TCCON differences has a different offset than the full dataset but a similar mean absolute error, station-to-station bias deviation and precision (Tables 2 and 3). The difference in the offset is mainly due to a difference in the sampling between the subset and the full dataset over the Northern Hemisphere. Due to few or no pairs occurring in Spring for the subset, the sampling misses the negative bias of the analysis there. Missing the negative bias of the analysis results in an increased offset. In that respect, the mean absolute error is less sensitive to the selection of pairs.

The analysis has a lower mean absolute error Δ than the one from the MACC GOSAT BESD data (0.65 ppm vs 1. ppm, Table 3), a station-to-station bias deviation σ almost half of the one from GOSAT data (0.7 ppm vs 1.3 ppm) and has an improved precision π (1 ppm vs 3.3 ppm). The mean correlation coefficient is also higher in the analysis than in the satellite data with a value of 0.8 compared to 0.5. The statistics of the MACC GOSAT BESD data found here are different than those of Heymann et al. (2015) who used a more recent version of the product. With the successive improvements in the BESD algorithm, the latest version has indeed a station-to-station bias deviation of ~ 0.4 ppm and a precision of ~ 2 ppm.

The better precision (lower value of π) and the lower value of the mean absolute error Δ and station-to-station bias deviation σ of the analysis compared to the MACC GOSAT BESD dataset shows that the analysis is capable of smoothing the scatter of the satellite data. Moreover, the analysis is able to fill the gaps of the satellite data in time and space.

5 Case study of a cold front over Park Falls

The CO$_2$ concentration could be strongly affected by frontal systems. As an illustration, such a situation occurred at the end of May 2013, close to the TCCON station of Park Falls, Wisconsin, USA, when a cold front came from the North-West. On 31 May, the XCO$_2$ dropped from 398.62 ppm at 08:15 LT to 395.97 ppm at 12:53 LT (Fig. 6, top panel). This sudden decrease of 2.65 ppm in less than 5 h occurs after the arrival of a cold front, which is associated with a decrease of the surface pressure and a decrease of the temperature at 500 hPa (Fig. 6, lower panel).

The free run is able to capture the sudden decrease in XCO$_2$, highlighting the ability of the model for such a situation (Fig. 6, upper panel). The flow during this period is mainly a descent of cold air from Canada towards the Midwestern and Eastern US. This cold air mass is depleted in CO$_2$ relative to the background (Fig. 7e and f). When it moves towards Park Falls, it results in decreasing XCO$_2$ as observed and simulated, but the decrease in the free run is too strong compared to the measurements.

We investigated whether the assimilation of the GOSAT data helps improve the simulated evolution of the CO$_2$ concentration for such situations even if the number of BESD GOSAT data is limited in the vicinity of a frontal system due to the strict cloud filtering. Frontal systems are associated with clouds formed when moist air between the cold and warm fronts is lifted.

On May, 30 we have a few GOSAT measurements over the North and North-East region of North America (Fig. 7a). These measurements have the effect of increasing the XCO$_2$ in this region (Fig. 7b–d). The cold air mass is then richer in CO$_2$ in the analysis compared to the free run, and when it moves towards Park Falls, the decrease is weaker and closer to the observed decrease. The assimilation of the GOSAT data helps improve the simulation by correcting the large scale structure upstream and by improving the large scale atmospheric CO$_2$ gradient.

The XCO$_2$ decrease continues the next day on 1 June in both simulations as the cold front continued its descent. Unfortunately, likely due to the presence of clouds, no TCCON measurements are available during this period to corroborate the simulated XCO$_2$ decrease.

6 Forecast based on the analysis

Within CAMS, we are receiving the GOSAT BESD data for a given day with a delay of 5 days behind real time. The analysis for this day is run as soon as the data are received. A 10 day forecast is then subsequently run based on the resulting analysis.

In this section, we aim ~~at evaluating~~ to evaluate the forecast as a function of ~~the~~ its lead time by comparing the forecast to the analysis valid for the same time. This comparison informs us about how long the information provided by the analysis lasts in the forecast. Assuming perfect transport and perfect surface fluxes, the analysis and the forecast (valid for the same time) should be similar given that the analysis ~~corrects accurately~~ accurately corrects the atmospheric concentration of CO$_2$. In practice, the differences ~~we will observe~~ observed between the analysis and the forecast ~~would~~ could either come from the transport, ~~from~~ the surface fluxes or ~~from~~ the analysis.

To compare a forecast with the analysis valid for the same time, we computed the anomaly correlation coefficient (ACC) for ~~the total column of~~ XCO$_2$ (see Appendix C for more details). The ACC can be regarded as a skill score relative to the climatology~~,~~: the higher the ACC, the better the forecast. In the framework of NWP, an ACC reaching 50 % corresponds to forecasts for which the error is the same as for a forecast based on a climatological average. An ACC of about 80 % indicates some skill in forecasting large-scale synoptic patterns.

We computed the ACC for each month individually as we know that the surface fluxes, drivers of the difference between the forecast and the analysis, have a strong seasonal cycle. We also computed it for different domains (globe, tropics and mid to high latitudes) and for several forecast lead times, from 12 h up to 10 days. We found that the ACC is globally more than 90 % for day 3 and almost always more than 85 % for day 5 for each single month (Fig. 38a). This means that the forecast for today based on the analysis of 5 days ago shows the same large-scale synoptic XCO$_2$ patterns as the analysis. The information of the analysis therefore lasts long enough in the forecast to provide a good quality forecast for today (compared to the analysis). The information lasts longer in the tropics than in the Northern Hemisphere and slightly longer in the Northern Hemisphere than in the Southern Hemisphere (Fig. 38b to d). This difference between the two hemispheres may reflect ~~that~~ the fact that the CO$_2$ variability is much weaker in the Southern Hemisphere.

For longer term forecasts, globally, there are two particular months for which the ACC decreases faster than the others, i.e. July and December. For example, for these two months the ACC at day 5 is similar to the ACC at day 10 for October. This means that for July and December, the medium range XCO$_2$ forecast should be used more carefully. For July, the drop in skill occurs mainly over the Northern Hemisphere. The main reason is that the CO$_2$ fluxes are an even more important driver of the CO$_2$ concentration than the initial CO$_2$ concentration for this month. To better understand the impact of the surface fluxes, let us assume that in July we have too little release or, similarly, too much uptake of CO$_2$ in the atmosphere in the model over the Northern Hemisphere (as confirmed by Fig. 32a). In the meantime, the analysis increases the CO$_2$ concentration helped by the GOSAT BESD

data (Fig. 35). ~~But~~ However, the next forecast will ~~decrease again~~ not increase enough the CO$_2$ concentration due to the ~~underestimation~~ negative bias of the CO$_2$ fluxes. This opposition between the analysis and the forecast explains the reduction in skill.

The global drop in skill for December is not directly related to a particular region as for July. It is nonetheless the second worst month for the tropics (after January) and the third worst for the Northern Hemisphere (together with September). Over the tropics during the winter, the reduction in skill is due to the opposite effect as for July over the Northern Hemisphere: the CO$_2$ fluxes are important and there is a positive bias in the fluxes (too much release or too little uptake of CO$_2$ in the atmosphere) in the model. For these situations when the CO$_2$ fluxes are the main driver of the atmospheric CO$_2$, the only solution to improve the skill would be to optimise the CO$_2$ fluxes together with the CO$_2$ initial conditions.

7   Conclusions

The Copernicus Atmosphere Monitoring Service (CAMS) greenhouse gases data assimilation within the Numerical Weather Prediction (NWP) framework of the Integrated Forecasting System (IFS) is designed to correct the atmospheric concentration of CO$_2$ instead of the surface fluxes in order to constrain the atmospheric CO$_2$. This requires the use of a short assimilation window so the error related to the model errors could be neglected. In the case of atmospheric CO$_2$, model errors are related to potentially inaccurate surface fluxes or transport.

This article demonstrates the benefit of the assimilation of ~~the~~ XCO$_2$ data derived from the Greenhouse gases Observing Satellite (GOSAT) by intermediate versions of the Bremen Optimal Estimation DOAS (BESD) algorithm of the University of Bremen (UoB). The assimilation of the GOSAT BESD XCO$_2$ provides a CO$_2$ analysis ~~which~~ that was compared to a free run forecast where the CO$_2$ concentration is not constrained by any CO$_2$ observation. The comparison was one year long (year 2013) and both simulations (analysis and free run) were evaluated against ~~the~~ measurements from the Total Carbon Column Observing Network (TCCON). We showed that the free run has a negative bias at northern mid-latitudes and a large positive bias in the tropical region with strong seasonal variations in both regions. These results are similar to those obtained with the same model and a similar configuration by Agustí-Panareda et al. (2014), where the causes of the bias are well detailed.

The analysis significantly reduces these biases without completely removing them with a remaining mean ~~bias~~ offset of $-$~~0.5~~0.34 ppm and a mean absolute error of 0.57 ppm compared to the TCCON data. However, the accuracy estimated with the station-to-station bias deviation is ~~0.7~~0.61 ppm. This represents a large improvement compared

to the free run for which the accuracy is 1.27 ppm. The precision of the analysis estimated with the mean scatter is 1.22 ppm, slightly better than for the free run with a value of 1.43 ppm.

The analysis was compared to the assimilated MACC GOSAT BESD data again using TCCON data as a reference. This comparison showed that the analysis has a lower station-to-station bias deviation than the assimilated data (0.7 ppm compared to 1.3 ppm). The precision is much better for the analysis, with a scatter of 1 ppm, while the assimilated data have a scatter of 3.3 ppm. The precision of the analysis is also better than the documented precision of other GOSAT XCO$_2$ products. The precision of the NIES product extracted from Yoshida et. al (2013) is 1.8 ppm. The precision of the Leicester and SRON products are respectively 2.5 ppm and 2.37 ppm (Dils et. al, 2014) . The CO$_2$ analysis is consequently an alternative to the XCO$_2$ GOSAT products as it provides a lower or similar station-to-station bias deviation and a better precision XCO$_2$ product compared to TCCON. Moreover, it does not have spatial and temporal gaps.

The pre-operational CAMS CO$_2$ analysis currently assimilates the most recent version of the GOSAT BESD data presented by Heymann et al. (2015) in near real time. These data have an improved bias deviation (~ 0.4 ppm) and an improved precision (~ 2 ppm) compared to those used in this study. The near real time CAMS CO$_2$ analysis should therefore have an improved station-to-station bias deviation and precision than the analysis presented in this paper.

We corrected the atmospheric concentration by only constraining the atmospheric concentration and not the surface fluxes. When and where the surface flux is a significant driver of the atmospheric concentration and if the assimilated data are not good enough or not numerous enough (in time and space), then constraining only atmospheric CO$_2$ does not compensate for the error in the surface flux. The next step is to further improve the carbon module CTESSEL in order to reduce the bias of the model. Another long term solution would be to constrain the surface flux at the same time as the concentration.

One strength of the CO$_2$ model used in this study is its ability to represent CO$_2$ variations associated with synoptic weather systems (Agustí-Panareda et al., 2014). By correcting the large scale XCO$_2$ patterns and removing part of the model bias, we showed with a case study that the analysis is able to better represent the CO$_2$ variations associated with these situations. The variations of the atmospheric reservoir of CO$_2$ are the result of changes in the surface fluxes to and from the atmosphere. If the characteristics of the analysis are found to be satisfactory, it could be included into a flux inversion system to infer surface fluxes.

The horizontal resolution of this study is about 80 km $\times$ 80 km while the horizontal resolution of the pre-operational analysis is 40 km $\times$ 40 km. One should expect an even better representation of the CO$_2$ variability in this analysis. In the future, the resolution could be increased even further toward the ECMWF operational resolution of about 16 km $\times$ 16 km.

The quality of the analysis is considered to be sufficient to assess the quality of the forecast as a function of its lead time. We showed that the forecast for day 3 and day 5, which will be the valid forecast range for today's forecast, has an anomaly correlation error of 90 and 85 %, respectively. This means that we are providing a CO$_2$ forecast with accurate synoptic features for today and for the next days. With a good representation of the variability and a bias mostly under 1 ppm, the CAMS atmospheric CO$_2$ promises to become a useful product, for example, for planning a measurement campaign. It could also be used as the a priori in the satellite or TCCON retrieval algorithms or be used to evaluate the retrieval products from the Orbiting Carbon Observatory-2 (OCO-2, oco.jpl.nasa.gov).

Appendix A: Comparing the model against TCCON

For the comparison with the TCCON data, one has to account for the a priori information used in the retrieval that links $\hat{c}^o$, the TCCON retrieved XCO$_2$ to $\boldsymbol{x}^{\mathrm{t}}$, the true (unknown) CO$_2$ profile (Wunch et al., 2011b),

$$\hat{c}^o = c^b + \boldsymbol{a}^{\mathrm{T}}\left(\boldsymbol{x}^{\mathrm{t}} - \boldsymbol{x}^b\right) + \varepsilon, \tag{A1}$$

where $\boldsymbol{x}^b$ is an a priori profile of CO$_2$, $\boldsymbol{a}$ is a vector resulting from the product of the averaging kernel matrix with a dry-pressure weighting function vector (for the vertical integration), c^b is the column-averaged mixing ratio computed from $\boldsymbol{x}^b$, and ε is the error in the retrieved column-averaged mixing ratio. This error includes the random and systematic errors in the measured signal and in the retrieval algorithm.

To compare the model with the TCCON retrieved value, we used the same a priori information, so that the model profile $\boldsymbol{x}$ is converted to a column-averaged mixing ratio $\hat{c}$ by

$$\hat{c} = c^b + \boldsymbol{a}^{\mathrm{T}}\left(\boldsymbol{x} - \boldsymbol{x}^b\right). \tag{A2}$$

The comparison between the simulation and TCCON occurs in the observation space with the difference between the model column-averaged mixing ratio $\hat{c}$ of Eq. (A2) and the TCCON column-averaged mixing ratio $\hat{c}^o$ of Eq. (A1),

$$\hat{c} - \hat{c}^o = \boldsymbol{a}^{\mathrm{T}}\left(\boldsymbol{x} - \boldsymbol{x}^{\mathrm{t}}\right) - \varepsilon. \tag{A3}$$

Let us define $\eta = \boldsymbol{a}^{\mathrm{T}}(\boldsymbol{x} - \boldsymbol{x}^{\mathrm{t}})$ as the model error in terms of the column-averaged mixing ratio. It accounts for

numerous errors, for example, the errors directly linked to the model processes like the transport, the errors in the surface fluxes, the ~~representativeness~~ representativity error and the error due to the assimilation of the GOSAT XCO$_2$ data for the analysis. The difference between the smooth model ~~column~~ column-averaged mixing ratio $\hat{c}$ and the TCCON ~~column~~ column-averaged mixing ratio $\hat{c}^o$ is therefore the sum of the model error η and the error in the retrieved ~~column~~ column-averaged mixing ratio ε.

To compute the model ~~column~~ column-averaged mixing ratio $\hat{c}$ of Eq. (A2) equivalent to each TCCON measurement, we extracted the two model profiles ~~which~~ that are closest to the measurement time and ~~which are~~ in the nearest grid point ~~of the station where the measurement was realised. Then we did a time interpolation of the two profiles in order to have to the measurement.~~ The two profiles are then interpolated in time in order to obtain the model profile at the same time as the measurement. Eventually, we computed the ~~column~~ column-averaged mixing ratio according to Eq. (A2).

Appendix B: Smoothing the statistics against TCCON

In order to have a more global view of the bias and the scatter of a simulation against the data from the TCCON network, we have developed and used a two-step algorithm. The first step consists in computing the statistics (bias and the standard deviation) for each week of 2013 and for each TCCON station when the ~~in situ~~ data are available. The weekly statistics are then interpolated in time using a function described in the following Sect. B1. This allows one to fill in the gaps in time when no data are available. We therefore have a value for the bias at each station and for each week. For the second step, we compute a quadratic function of latitude that best fits the interpolated biases for each week (Sect. B2).

B1 Time smoothing

For each TCCON station ~~we aggregate per week the measurements and their equivalent from the simulation. For each week when more than 10 measurements are available~~ k and for each week w^l for $l \in [1, 52]$, we compute the ~~average and~~ mean difference δ_k^l and the standard deviation of the difference ~~between every model value and observation, in the observation space~~ σ_k^l between every TCCON observation during this week and the model equivalent value. The statistics are computed only when more than 10 measurements are available during the week. The averaged difference (or bias) is then interpolated in time t with the function ~~$\tilde{b}(t)$~~ $\tilde{b}_k(t)$ that combines a linear growth and a harmonic component,

$$\tilde{b}_k(t) = a_k\, t + b_k + \alpha_k \sin\left(\frac{t}{\tau_1} + \varphi_k\right) + \beta_k \sin\left(\frac{t}{\tau_2} + \varphi_k\right).$$

(B1)

~~a, b, α, β and φ~~ a_k, b_k, α_k, β_k and φ_k are the parameters of the function ~~$\tilde{b}(t)$~~ $\tilde{b}_k(t)$ obtained by an optimisation procedure that minimises the distance between ~~$\tilde{b}(t)$ and the raw bias~~ $\tilde{b}_k(t)$ and the series of δ_k^l for $l \in [1, 52]$. τ_1 is chosen to be 6 months and τ_2 3 months. The form of the function of Eq. (B1) thus gives a linear growing bias and allows seasonal variations. A similar function is used for the standard deviation.

B2 Spatial smoothing

The time smoothing allows us to fill in the gaps in the time series of the bias for each station, when for one week we do not have any measurement to compare with. Following Bergamaschi et al. (2009), we then compute for each week w^l the best fit of the interpolated biases with a quadratic function of latitude ~~$\hat{b}$,~~ $\hat{b}^l$,

$$\hat{b}^l(\phi) = a^l \phi^2 + b^l \phi + c^l,$$

(B2)

with ϕ is the sine of the latitude. ~~a, b and c~~ a^l, b^l and c^l are obtained by an optimisation procedure that minimises the distance between ~~$\hat{b}$~~ $\hat{b}^l$ and the weekly interpolated biases δ_k^l for $k \in [1, N]$. A similar function is used for the standard deviation.

B3 Discussion

For some stations, the availability of the weekly differences is not well spread in time and the time smoothing of Eq. B1 provides spurious values. We solved this issue by fixing the coefficient α_k to a zero value (See Table S1 of the Supplement).

With a root mean square error (RMSE) mostly under 0.7 ppm and a correlation mostly over 0.8, the smoothed bias matches well with the weekly bias (Table S1 of the Supplement). The Hovmöller diagram can be considered as an accurate representation of the overall bias.

Compared to the bias, the fit between the time series of the weekly scatter and the regression is not as good for the scatter. The correlation coefficient is mostly between 0.5 and 0.7 (Table S1 of the Supplement).

Appendix C: Anomaly correlation coefficient

The anomaly correlation coefficient ACC between the forecast f and the analysis a is computed using the climatology c by

$$\mathrm{ACC} = \frac{\overline{(f - c)(a - c)}}{\sqrt{\overline{(f - c)^2}\,\overline{(a - c)^2}}},$$

(C1)

where the overline, is the spatial and temporal average. For example, for the forecast range 24 hr, we take the XCO$_2$

fields from all the 24 hr forecasts for a given month, all the analyses valid for the same time, and a fixed climatology for this month.

The climatology is based on a free run simulation using the optimised CO$_2$ surface fluxes from Chevallier et al. (2010) which simulated the years from 2003 to 2012. For each month, we compute the average over the 10 years of the simulation, rescaling the mean so that the mean is the same as for the analysis, avoiding by this procedure the issue of the increase in CO$_2$ over time. The two dimensional climatology field for XCO$_2$ for the month m is

$$c(m) = \frac{1}{10} \sum_{y=2003}^{2012} \frac{1}{n(y,m)} \sum_{d=1}^{n(y,m)} \left[\Sigma(y,m,d) - \overline{\Sigma}(y,m,d) \right] + \overline{\Sigma}_{an}(m) \tag{C2}$$

where y is the year, n the number of days for the year y and the month m, d is an index for the day, $\Sigma(y,m,d)$ is the XCO$_2$ field from the simulation for the year y, the month m and the day d, $\overline{\Sigma}$ is a spatial average of Σ and $\overline{\Sigma}_{an}(m)$ is the spatial and temporal average of the XCO$_2$ fields from the analysis for the month m (and the year 2013).

The Supplement related to this article is available online at doi:10.5194/acp-0-1-2015-supplement.

Author contributions. S. Massart designed and carried out the experiments with the help of A. Agustí-Panareda and advice from F. Chevallier, J. Heymann and M. Buchwitz. J. Heymann, M. Reuter, M. Hilker, M. Buchwitz and J. P. Burrows have been responsible for the design and operation of the BESD GOSAT XCO$_2$ retrieval algorithm. S. Massart prepared the manuscript with contributions from A. Agustí-Panareda, J. Heymann, M. Buchwitz, F. Chevallier, M. Reuter, M. Hilker, J.P. Burrows, D. G. Feist, and F. Hase. N. M. Deutscher and R. Sussmann contributed to the ACP version of the paper. F. Desmet is the co-investigator of the La Réunion TCCON station. N. M. Deutscher and C. Petri are responsible for the Białystok, Bremen and Orléans TCCON data M. Dubey is the PI of Four Corners TCCON station. D. G. Feist is the PI of the Ascension TCCON station. D. W. T. Griffith and V. Velazco are the PIs of Darwin and Wollongong stations. F. Hase is the PI of the Karlsruhe TCCON station. R. Kivi is the PI of the Sodankylä TCCON station. M. Schneider is the PI of Izaña TCCON station. R. Sussmann is the PI of the Garmisch TCCON station.

References

Agustí-Panareda, A., Massart, S., Boussetta, S., Balsamo, G., Beljaars, A., Chevallier, F., Engelen, R., Peuch, V.-H., and Razinger, M.: The new MACC-II CO$_2$ forecast, ECMWF Newsletter, 135, 8–13, 2013.

Agustí-Panareda, A., Massart, S., Chevallier, F., Boussetta, S., Balsamo, G., Beljaars, A., Ciais, P., Deutscher, N. M., Engelen, R., Jones, L., Kivi, R., Paris, J.-D., Peuch, V.-H., Sherlock, V., Vermeulen, A. T., Wennberg, P. O., and Wunch, D.: Forecasting global atmospheric CO$_2$, Atmos. Chem. Phys., 14, 11959–11983, doi:10.5194/acp-14-11959-2014, 2014.

Bergamaschi, P., Frankenberg, C., Meirink, J. F., Krol, M., Villani, M. G., Houweling, S., Dentener, F., Dlugokencky, E. J., Miller, J. B., Gatti, L. V., Engel, A., and Levin, I.: Inverse modeling of global and regional CH$_4$ emissions using SCIAMACHY satellite retrievals, J. Geophys. Res.-Atmos., 114, D22301, doi:10.1029/2009JD012287, 2009.

Blumenstock, T., Hase, F., Schneider, M., García, O. E., and Sepúlveda, E.: TCCON data from Izana, Tenerife, Spain, Release GGG2014R0, TCCON data archive, hosted by the Carbon Dioxide Information Analysis Center, Oak Ridge National Laboratory, Oak Ridge, Tennessee, USA, doi:10.14291/tccon.ggg2014.izana01.R0/1149295, 2014.

Boussetta, S., Balsamo, G., Beljaars, A., Agusti-Panareda, A., Calvet, J.-C., Jacobs, C., van den Hurk, B., Viterbo, P., Lafont, S., Dutra, E., Jarlan, L., Balzarolo, M., Papale, D., and van der Werf, G.: Natural carbon dioxide exchanges in the ECMWF integrated forecasting system: implementation and offline validation, J. Geophys. Res.-Atmos., 118, 1–24, doi:10.1002/jgrd.50488, 2013.

Chédin, A., Saunders, R., Hollingsworth, A., Scott, N., Matricardi, M., Etcheto, J., Clerbaux, C., Armante, R., and Crevoisier, C.: The feasibility of monitoring CO$_2$ from high-resolution infrared sounders, J. Geophys. Res.-Atmos., 108, 4064, doi:10.1029/2001JD001443, 2003.

Chevallier, F., Ciais, P., Conway, T. J., Aalto, T., Anderson, B. E., Bousquet, P., Brunke, E. G., Ciattaglia, L., Esaki, Y., Fröhlich, M., Gomez, A., Gomez-Pelaez, A. J., Haszpra, L., Krummel, P. B., Langenfelds, R. L., Leuenberger, M., Machida, T., Maignan, F., Matsueda, H., Morguí, J. A., Mukai, H., Nakazawa, T., Peylin, P., Ramonet, M., Rivier, L., Sawa, Y.,

Schmidt, M., Steele, L. P., Vay, S. A., Vermeulen, A. T., Wofsy, S., and Worthy, D.: CO$_2$ surface fluxes at grid point scale estimated from a global 21 year reanalysis of atmospheric measurements, J. Geophys. Res.-Atmos., 115, D21307, doi:10.1029/2010JD013887, 2010.

Ciais, P., Sabine, C., Bala, G., Bopp, L., Brovkin, V., Canadell, J., Chhabra, A., DeFries, R., Galloway, J., Heimann, M., Jones, C., Quéré, C. L., Myneni, R., Piao, S., and Thornton, P.: Climate change 2013: the physical science basis, in: Contribution of Working Group I to the Fifth Assessment Report of the Intergovernmental Panel on Climate Change, edited by: Stocker, T. F., Qin, D., Plattner, G.-K., Tignor, M., Allen, S. K., Boschung, J., Nauels, A., Xia, Y., Bex, V., and Midgley, P. M., chap. Carbon and Other Biogeochemical Cycles, Cambridge University Press, Cambridge, UK and New York, NY, USA, 465–570, 2013.

De Maziere, M., Desmet, F., Hermans, C., Scolas, F., Kumps, N., Metzger, J.-M., Duflot, V., and Cammas, J.-P.: TCCON data from Reunion Island (La Reunion), France, Release GGG2014R0, TCCON data archive, hosted by the Carbon Dioxide Information Analysis Center, Oak Ridge National Laboratory, Oak Ridge, Tennessee, USA, doi:10.14291/tccon.ggg2014.reunion01.R0/1149288, 2014.

Deutscher, N., Notholt, J., Messerschmidt, J., Weinzierl, C., Warneke, T., Petri, C., Grupe, P., and Katrynski, K.: TCCON data from Bialystok, Poland, Release GGG2014R0, TCCON data archive, hosted by the Carbon Dioxide Information Analysis Center, Oak Ridge National Laboratory, Oak Ridge, Tennessee, USA, doi:10.14291/tccon.ggg2014.bialystok01.R0/1149277, 2014.

Dils, B., Buchwitz, M., Reuter, M., Schneising, O., Boesch, H., Parker, R., Guerlet, S., Aben, I., Blumenstock, T., Burrows, J. P., Butz, A., Deutscher, N. M., Frankenberg, C., Hase, F., Hasekamp, O. P., Heymann, J., De Mazière, M., Notholt, J., Sussmann, R., Warneke, T., Griffith, D., Sherlock, V. and Wunch, D.: The Greenhouse Gas Climate Change Initiative (GHG-CCI): comparative validation of GHG-CCI SCIAMACHY/ENVISAT and TANSO-FTS/GOSAT CO$_2$ and CH$_4$ retrieval algorithm products with measurements from the TCCON, Atmos. Meas. Tech., 7, 1723–1744, 2014.

Dubey, M., Lindenmaier, R., Henderson, B., Green, D., Allen, N., Roehl, C., Blavier, J.-F., Butterfield, Z., Love, S., Hamelmann, J., Wunch. D.: TCCON data from Four Corners, NM, USA, Release GGG2014R0. TCCON data archive, hosted by the Carbon Dioxide Information Analysis Center, Oak Ridge National Laboratory, Oak Ridge, Tennessee, U.S.A. doi:10.14291/tccon.ggg2014.fourcorners01.R0/1149272 2014.

Engelen, R. J., Serrar, S., and Chevallier, F.: Four-dimensional data assimilation of atmospheric CO$_2$ using AIRS observations, J. Geophys. Res.-Atmos., 114, D03303, doi:10.1029/2008JD010739, 2009.

Feist, D. G., Arnold, S. G., John, N., and Geibel, M. C.: TCCON data from Ascension Island, Saint Helena, Ascension and Tristan da Cunha, Release GGG2014R0, TCCON data archive, hosted by the Carbon Dioxide Information Analysis Center, Oak Ridge National Laboratory, Oak Ridge, Tennessee, USA, doi:10.14291/tccon.ggg2014.ascension01.R0/1149285, 2014.

Griffith, D. W. T., Deutscher, N., Velazco, V. A., Wennberg, P. O., Yavin, Y., Aleks, G. K., Washenfelder, R., Toon, G. C., Blavier, J.-F., Murphy, C., Jones, N., Kettlewell, G., Connor, B.,

Macatangay, R., Roehl, C., Ryczek, M., Glowacki, J., Culgan, T., and Bryant, G.: TCCON data from Darwin, Australia, Release GGG2014R0, TCCON data archive, hosted by the Carbon Dioxide Information Analysis Center, Oak Ridge National Laboratory, Oak Ridge, Tennessee, USA, doi:10.14291/tccon.ggg2014.darwin01.R0/1149290, 2014a.

Griffith, D. W. T., Velazco, V. A., Deutscher, N., Murphy, C., Jones, N., Wilson, S., Macatangay, R., Kettlewell, G., Buchholz, R. R., and Riggenbach, M.: TCCON data from Wollongong, Australia, Release GGG2014R0, TCCON data archive, hosted by the Carbon Dioxide Information Analysis Center, Oak Ridge National Laboratory, Oak Ridge, Tennessee, USA, doi:10.14291/tccon.ggg2014.wollongong01.R0/1149291, 2014b.

Hase, F., Blumenstock, T., Dohe, S., Groß, J., and Kiel, M.: TCCON data from Karlsruhe, Germany, Release GGG2014R1, TCCON data archive, hosted by the Carbon Dioxide Information Analysis Center, Oak Ridge National Laboratory, Oak Ridge, Tennessee, USA, doi:10.14291/tccon.ggg2014.karlsruhe01.R1/1182416, 2014.

Heymann, J., Reuter, M., Hilker, M., Buchwitz, M., Schneising, O., Bovensmann, H., Burrows, J. P., Kuze, A., Suto, H., Deutscher, N. M., Dubey, M. K., Griffith, D. W. T., Hase, F., Kawakami, S., Kivi, R., Morino, I., Petri, C., Roehl, C., Schneider, M., Sherlock, V., Sussmann, R., Velazco, V. A., Warneke, T., and Wunch, D.: Consistent satellite XCO$_2$ retrievals from SCIAMACHY and GOSAT using the BESD algorithm, Atmos. Meas. Tech. Discuss., 8, 1787–1832, doi:10.5194/amtd-8-1787-2015, 2015.

Kawakami, S., Ohyama, H., Arai, K., Okumura, H., Taura, C., Fukamachi, T., and Sakashita, M.: TCCON data from Saga, Japan, Release GGG2014R0, TCCON data archive, hosted by the Carbon Dioxide Information Analysis Center, Oak Ridge National Laboratory, Oak Ridge, Tennessee, USA, doi:10.14291/tccon.ggg2014.saga01.R0/1149283, 2014.

Kivi, R., Heikkinen, P., and Kyro, E.: TCCON data from Sodankyla, Finland, Release GGG2014R0., TCCON data archive, hosted by the Carbon Dioxide Information Analysis Center, Oak Ridge National Laboratory, Oak Ridge, Tennessee, USA, doi:10.14291/tccon.ggg2014.sodankyla01.R0/1149280, 2014.

Kuze, A., Suto, H., Nakajima, M. and Hamazaki, T.: Thermal and near infrared sensor for carbon observation Fourier-transform spectrometer on the Greenhouse Gases Observing Satellite for greenhouse gases monitoring, Applied Optics, 48, 6716–6733, 2009.

Massart, S., Agusti-Panareda, A., Aben, I., Butz, A., Chevallier, F., Crevoisier, C., Engelen, R., Frankenberg, C., and Hasekamp, O.: Assimilation of atmospheric methane products into the MACC-II system: from SCIAMACHY to TANSO and IASI, Atmos. Chem. Phys., 14, 6139–6158, doi:10.5194/acp-14-6139-2014, 2014.

Notholt, J., Petri, C., Warneke, T., Deutscher, N., Buschmann, M., Weinzierl, C., Macatangay, R., Grupe. P.: TCCON data from Bremen, Germany, Release GGG2014R0. TCCON data archive, hosted by the Carbon Dioxide Information Analysis Center, Oak Ridge National Laboratory, Oak Ridge, Tennessee, U.S.A. doi:10.14291/tccon.ggg2014.bremen01.R0/1149275, 2014.

Parrish, D. and Derber, J.: National Meteorological Center's spectral statistical interpolation analysis system, Mon. Weather Rev., 120, 1747–1763, 1992.

Reuter, M., Buchwitz, M., Schneising, O., Heymann, J., Bovensmann, H., and Burrows, J. P.: A method for improved SCIA-MACHY CO$_2$ retrieval in the presence of optically thin clouds, Atmos. Meas. Tech., 3, 209–232, doi:10.5194/amt-3-209-2010, 2010.

Reuter, M., Bovensmann, H., Buchwitz, M., Burrows, J. P., Connor, B. J., Deutscher, N. M., Griffith, D. W. T., Heymann, J., Keppel-Aleks, G., Messerschmidt, J., Notholt, J., Petri, C., Robinson, J., Schneising, O., Sherlock, V., Velazco, V., Warneke, T., Wennberg, P. O., and Wunch, D.: Retrieval of atmospheric CO$_2$ with enhanced accuracy and precision from SCIAMACHY: validation with FTS measurements and comparison with model results, J. Geophys. Res.-Atmos., 116, D04301, doi:10.1029/2010JD015047, 2011.

Sherlock, V. B., Connor, Robinson, J., Shiona, H., Smale, D., and Pollard, D.: TCCON data from Lauder, New Zealand, 125HR, Release GGG2014R0, TCCON data archive, hosted by the Carbon Dioxide Information Analysis Center, Oak Ridge National Laboratory, Oak Ridge, Tennessee, USA, doi:10.14291/tccon.ggg2014.lauder02.R0/1149298, 2014.

Sussmann, R. and Rettinger, M.: TCCON data from Garmisch, Germany, Release GGG2014R0, TCCON data archive, hosted by the Carbon Dioxide Information Analysis Center, Oak Ridge National Laboratory, Oak Ridge, Tennessee, USA, doi:10.14291/tccon.ggg2014.garmisch01.R0/1149299, 2014.

Wang, J.-W., Denning, A. S., Lu, L., Baker, I. T., Corbin, K. D., and Davis, K. J.: Observations and simulations of synoptic, regional, and local variations in atmospheric CO$_2$, J. Geophys. Res.-Atmos., 112, D04108, doi:10.1029/2006JD007410, 2007.

Warneke, T., Messerschmidt, J., Notholt, J., Weinzierl, C., Deutscher, N., Petri, C., Grupe, P., Vuillemin, C., Truong, F., Schmidt, M., Ramonet, M., and Parmentier, E.: TCCON data from Orleans, France, Release GGG2014R0, TCCON data archive, hosted by the Carbon Dioxide Information Analysis Center, Oak Ridge National Laboratory, Oak Ridge, Tennessee, USA, doi:10.14291/tccon.ggg2014.orleans01.R0/1149276, 2014.

Wennberg, P. O., Roehl, C., Wunch, D., Toon, G. C., Blavier, J.-F., Washenfelder, R., Keppel-Aleks, G., Allen, N., and Ayers, J.: TCCON data from Park Falls, Wisconsin, USA, Release GGG2014R0, TCCON data archive, hosted by the Carbon Dioxide Information Analysis Center, Oak Ridge National Laboratory, Oak Ridge, Tennessee, USA, doi:10.14291/tccon.ggg2014.parkfalls01.R0/1149161, 2014a.

Wennberg, P. O., Wunch, D., Roehl, C., Blavier, J.-F., Toon, G. C., Allen, N., Dowell, P., Teske, K., Martin, C., and Martin, J.: TCCON data from Lamont, Oklahoma, USA, Release GGG2014R0, TCCON data archive, hosted by the Carbon Dioxide Information Analysis Center, Oak Ridge National Laboratory, Oak Ridge, Tennessee, USA, doi:10.14291/tccon.ggg2014.lamont01.R0/1149159, 2014b.

Wunch, D., Toon, G. C., Blavier, J.-F. L., Washenfelder, R. A., Notholt, J., Connor, B. J., Griffith, D. W. T., Sherlock, V., and Wennberg, P. O.: The total carbon column observing network, Philos. T. Roy. Soc. A, 369, 2087–2112, doi:10.1098/rsta.2010.0240, 2011a.

Wunch, D., Wennberg, P. O., Toon, G. C., Connor, B. J., Fisher, B., Osterman, G. B., Frankenberg, C., Mandrake, L., O'Dell, C., Ahonen, P., Biraud, S. C., Castano, R., Cressie, N., Crisp, D., Deutscher, N. M., Eldering, A., Fisher, M. L., Griffith, D. W. T., Gunson, M., Heikkinen, P., Keppel-Aleks, G., Kyrö, E., Lindenmaier, R., Macatangay, R., Mendonca, J., Messerschmidt, J., Miller, C. E., Morino, I., Notholt, J., Oyafuso, F. A., Rettinger, M., Robinson, J., Roehl, C. M., Salawitch, R. J., Sherlock, V., Strong, K., Sussmann, R., Tanaka, T., Thompson, D. R., Uchino, O., Warneke, T., and Wofsy, S. C.: A method for evaluating bias in global measurements of CO$_2$ total columns from space, Atmos. Chem. Phys., 11, 12317–12337, doi:10.5194/acp-11-12317-2011, 2011b.

Yoshida, Y., Kikuchi, N., Morino, I., Uchino, O., Oshchepkov, S., Bril, A., Saeki, T., Schutgens, N., Toon, G. C., Wunch, D., Roehl, C. M., Wennberg, P. O., Griffith, D. W. T., Deutscher, N. M., Warneke, T., Notholt, J., Robinson, J., Sherlock, V., Connor, B., Rettinger, M., Sussmann, R., Ahonen, P., Heikkinen, P., Kyrö, E., Mendonca, J., Strong, K., Hase, F., Dohe, S. and Yokota, T.: Improvement of the retrieval algorithm for GOSAT SWIR XCO$_2$ and XCH$_4$ and their validation using TCCON data, Atmos. Meas. Tech., 6, 1533–1547, 2013.

Table 31. List on the used TCCON stations ordered by latitude from North to South.

Site	Lat	Lon	Starting date	Reference
Sodankylä (sodankyla01)	67.37	26.63	6 Feb 2009	Kivi et al. (2014)
Białystok (bialystok01)	53.23	23.02	1 ~~Mar2009~~ Mar 2009	Deutscher et al. (2014)
Bremen (bremen01)	53.10	8.85	6 Jan 2005	Notholt et al. (2014)
Karlsruhe (karlsruhe01)	49.10	8.44	19 Apr 2010	Hase et al. (2014)
Orléans (orleans01)	47.97	2.11	29 Aug 2009	Warneke et al. (2014)
Garmisch (garmisch01)	47.48	11.06	16 Jul 2007	Sussmann and Rettinger (2014)
Park Falls (parkfalls01)	45.94	−90.27	26 May 2004	Wennberg et al. (2014a)
Four Corners (fourcorners01)	36.80	−108.48	1 Mar 2011	Dubey et al. (2014)
Lamont (lamont01)	36.60	−97.49	6 Jul 2008	Wennberg et al. (2014b)
Saga (saga01)	33.24	130.29	28 Jul 2011	Kawakami et al. (2014)
Izaña (izana01)	28.30	−16.48	18 May 2007	Blumenstock et al. (2014)
Ascension Island (ascension01)	−7.92	−14.33	22 May 2012	Feist et al. (2014)
Darwin (darwin01)	−12.43	130.89	28 Aug 2005	Griffith et al. (2014a)
~~Reunion~~ Réunion Island (reunion01)	−20.90	55.49	6 Oct 2011	De Maziere et al. (2014)
Wollongong (wollongong01)	−34.41	150.88	26 Jun 2008	Griffith et al. (2014b)
Lauder 125HR (lauder02)	−45.05	169.68	2 Feb 2010	Sherlock et al. (2014)

Table 32. Statistics of the XCO$_2$ difference between the simulations (free run and analysis) and the average hourly TCCON data (model-TCCON): bias (δ_k, in ppm), scatter (σ_k, in ppm) and correlation coefficient (r_k). Also shown are the mean, the mean absolute error (MAE) and the deviation of the stations bias (respectively δ, Δ and σ), the mean scatter (π) and the mean r (last three rows). The second column (N) is the number of data used for computing the statistics.

Site	N	Free run			Analysis		
		Bias	Scatter	r	Bias	Scatter	r
Sodankylä	20441	−1.59	1.35	0.91	−0.55	1.35	0.92
Białystok	16063	−2.68	1.96	0.81	−1.66	1.80	0.77
Bremen	4883	−1.62	1.52	0.79	−0.41	1.27	0.82
Karlsruhe	4201	−1.26	1.72	0.80	−0.25	1.54	0.82
Orléans	8444	−0.38	1.36	0.85	0.09	1.21	0.91
Garmisch	10371	−0.92	1.59	0.82	−0.29	1.62	0.80
Park Falls	27991	−1.69	2.06	0.81	−0.60	1.45	0.90
Four Corners	19872	0.69	1.76	0.58	0.57	1.43	0.74
Lamont	43731	−0.20	2.09	0.59	0.04	1.35	0.80
Saga	10349	−1.19	1.61	0.75	−0.64	1.33	0.83
Izaña	4463	0.27	0.80	0.90	0.40	0.62	0.94
Ascension Island	7111	2.31	1.29	0.24	0.72	1.27	0.21
Darwin	29194	1.57	1.12	0.78	−0.02	1.04	0.79
Réunion Island	18880	0.56	0.73	0.76	−0.77	0.60	0.78
Wollongong	27562	0.30	1.05	0.71	−1.08	1.06	0.65
Lauder	53500	0.01	0.83	0.86	−0.97	0.59	0.85
Mean	16	−0.36	1.43	0.75	−0.34	1.22	0.78
MAE	16	1.08	–	–	0.57	–	–
Deviation	16	1.27	–	–	0.61	–	–

Table 33. Statistics of the XCO$_2$ differences between the MACC GOSAT BESD dataset and the average hourly TCCON data (left block, GOSAT-TCCON) or the analysis and the average hourly TCCON data (right block, model-TCCON): ~~mean difference (~~bias (δ_k, in ppm), ~~standard deviation (~~scatter (σ_k, in ppm) and correlation coefficient (~~r~~r_k). The analysis has been sampled similarly to the GOSAT dataset in time and space. Also shown are the mean, the mean absolute error (MAE) and the deviation of the stations bias, the mean scatter and the mean r (last ~~two~~ three rows). The second column (N) is the number of data points used for computing the statistics.

| Site	N	MACC GOSAT dataset			Analysis		
		Bias	Scatter	r	Bias	Scatter	r
Sodankylä	90	−0.26	4.50	0.39	0.24	1.41	0.92
Białystok	~~73~~ 58	~~0.23~~ −0.28	~~3.35~~ 3.45	~~0.25~~ 0.32	~~1.00~~ 1.06	~~1.79~~ 1.99	~~0.35~~ 0.17
Bremen	41	1.19	2.34	0.53	0.54	0.86	0.81
Karlsruhe	~~94~~ 91	~~0.62~~ 1.45	2.74	~~0.53~~ 0.52	~~0.16~~ 0.89	~~0.79~~ 0.74	~~0.86~~ 0.88
Orléans	52	0.20	2.44	0.34	1.29	0.57	0.84
Garmisch	76	1.64	3.10	0.55	1.17	1.06	0.77
Park Falls	63	1.50	3.22	0.71	−0.08	1.03	0.95
Four Corners	102	−0.00	3.79	0.64	0.65	0.81	0.89
Lamont	340	−1.01	4.05	0.57	0.05	1.01	0.91
Saga	61	0.40	2.95	0.76	0.14	0.88	0.90
Darwin	234	−1.27	3.37	0.42	−0.11	0.81	0.84
Wollongong	221	−3.03	3.86	0.31	~~−1.17~~ 1.54	~~0.95~~ 1.07	~~0.79~~ 0.74
Mean	~~10~~ 12	~~−0.10~~ 0.04	~~3.36~~ 3.32	~~0.48~~ 0.50	~~0.27~~ 0.36	~~1.03~~ 1.02	~~0.81~~ 0.80
MAE	12	1.02	–	–	0.65	–	–
Deviation	~~10~~ 12	~~1.32~~ 1.31	–	–	~~0.69~~ 0.74	–	–
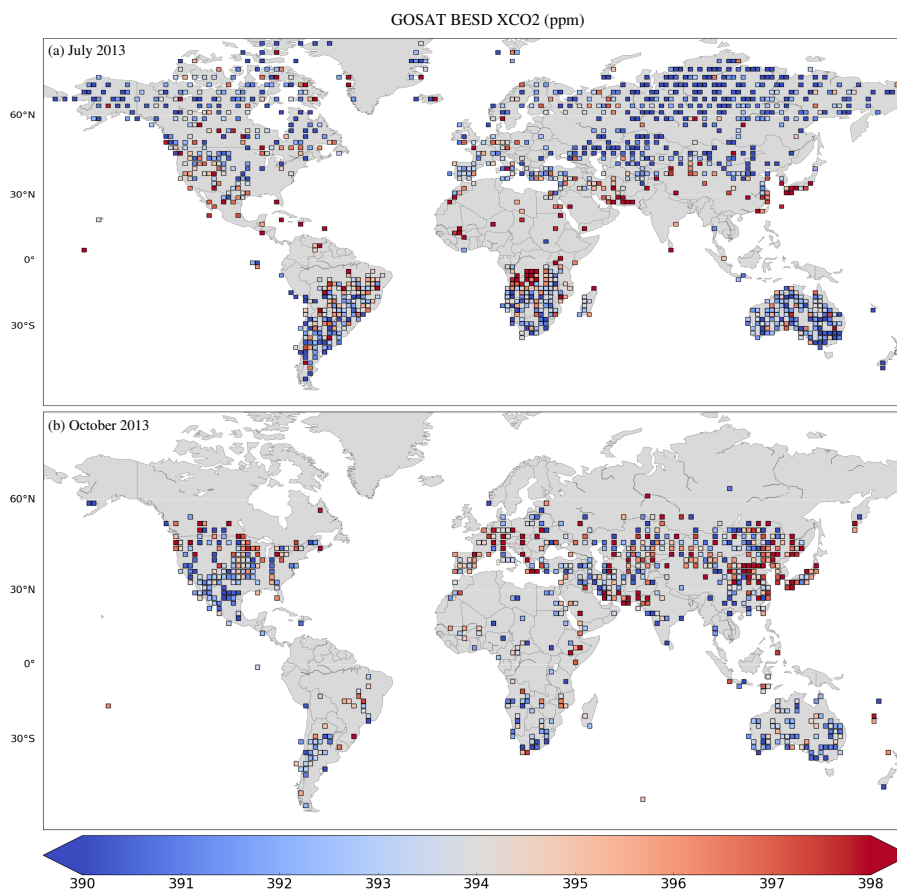
Figure 31. Example of the distribution of the assimilated GOSAT BESD XCO$_2$ data: July 2013 (top panel, about 3400 ~~data~~retrievals) and October 2013 (bottom, about 1270 ~~data~~retrievals). The monthly data are here aggregated on a $2° \times 2°$ grid and averaged. The blue/red represents the low/high averaged XCO$_2$ values in ppm.
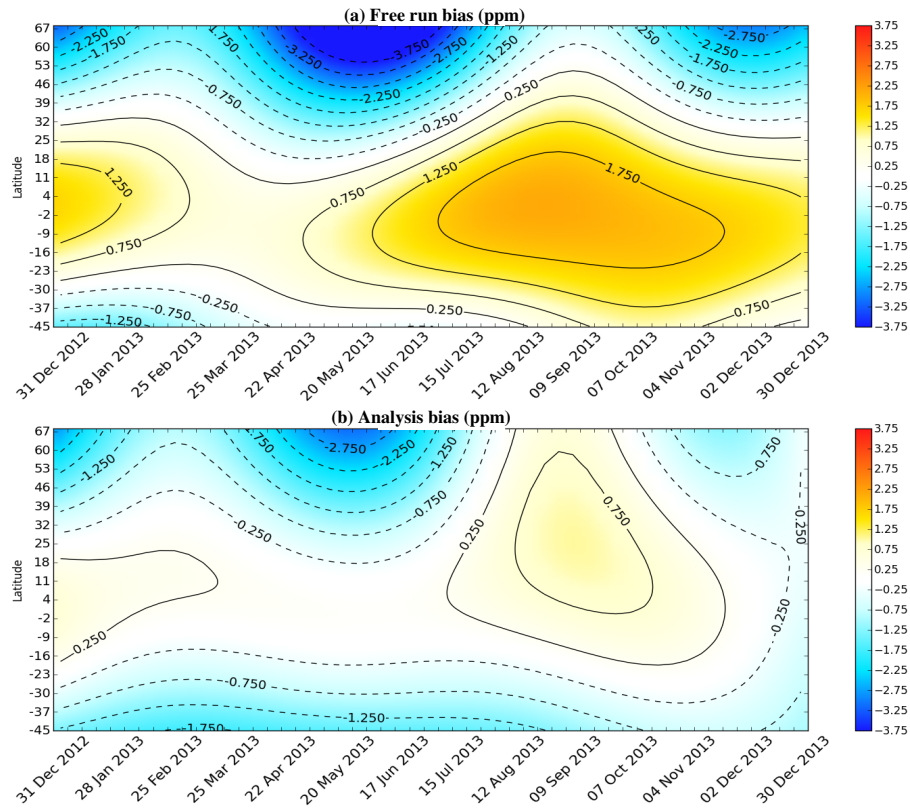
Figure 32. Hovmöller diagram (latitude vs. time) of the smoothed bias (in ppm, negative/positive in blue/red) of the simulated XCO_2 against the data of the TCCON network. Top: free run simulation. Bottom: analysis.
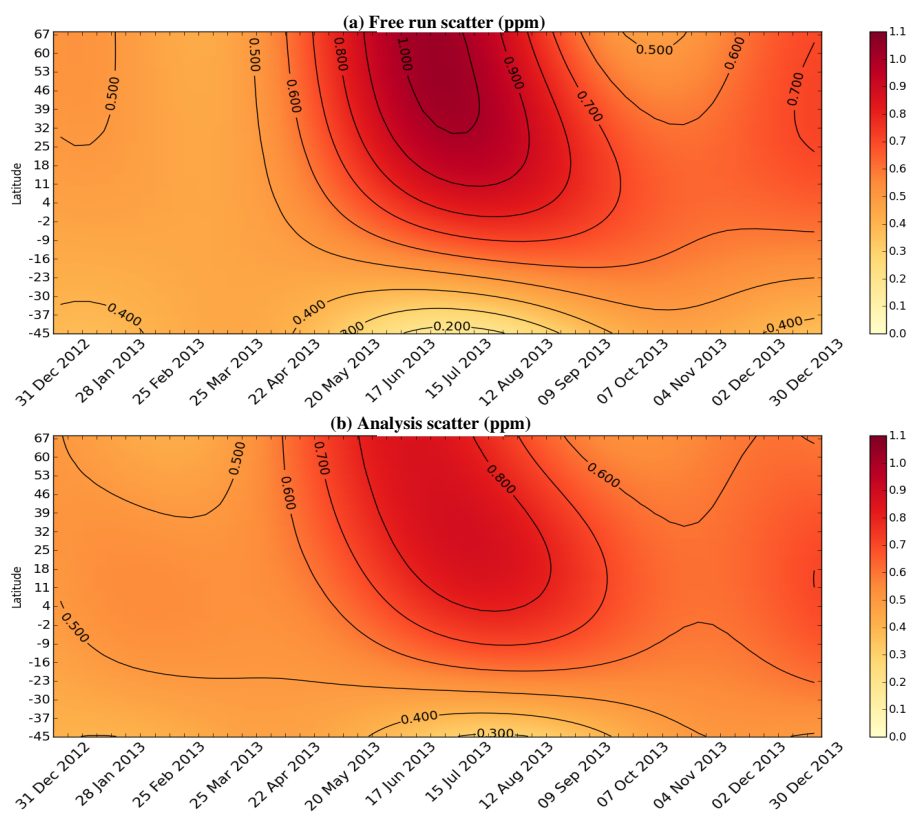
Figure 33. Same as Fig. 32 but for the standard deviation and yellow/red for low/high values.
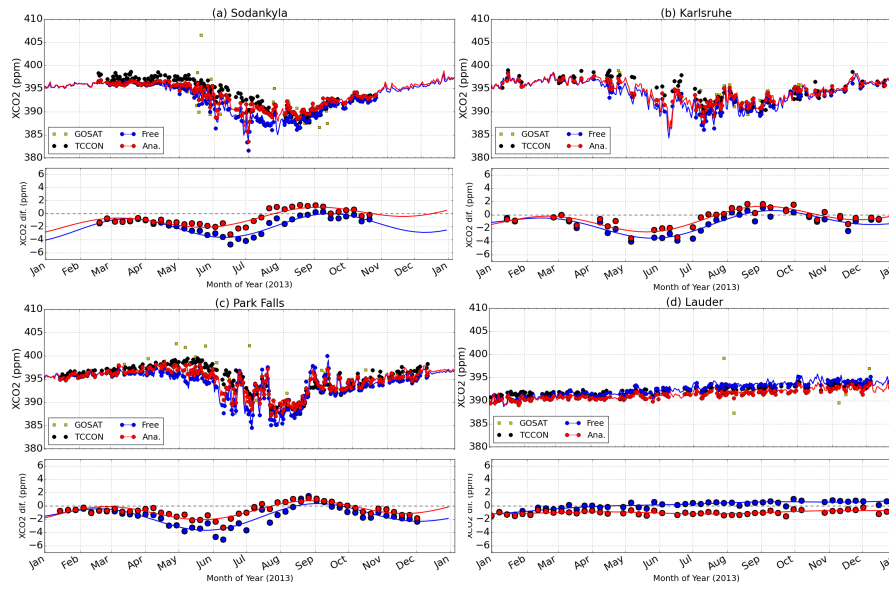
Figure 34. Time series of XCO$_2$ (in ppm) at **(a)** Sodankylä, **(b)** Karlsruhe, **(c)** Park Falls and ~~(c)~~ **(d)** Lauder. For each station, the top panel presents the daily averaged data from TCCON (black dots), the daily averaged data from GOSAT co-located in time and space with the station (yellow squares), the simulated XCO$_2$ (solid lines) and the daily averaged simulated XCO$_2$ in the observation space (coloured dots). The bottom panel presents the weekly averaged bias of the simulated XCO$_2$ against the TCCON data (coloured dots) and the smoothed bias (solid lines). The blue colour is for the free run while the red colour is for the analysis.
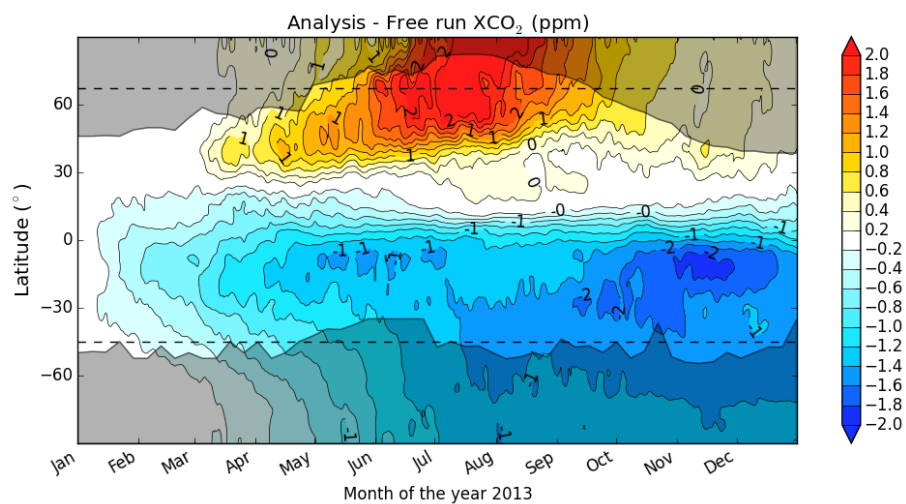
Figure 35. Hovmöller diagram (latitude vs. time) of the difference in ppm (negative/positive in blue/red) between XCO$_2$ from the analysis and from the free run simulation. The horizontal dotted lines represent the latitude of the northernmost and the southernmost TCCON station respectively. The grey shaded areas are where GOSAT does not provide observations.
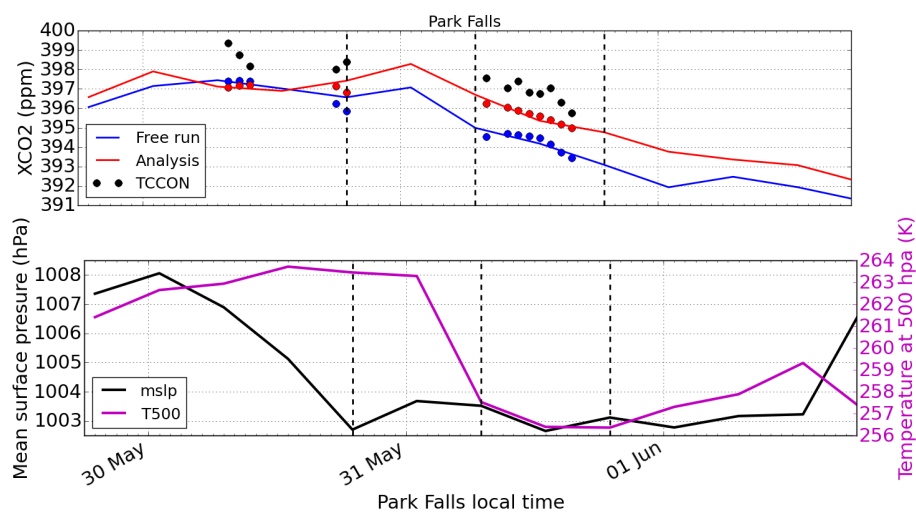
Figure 36. Situation over Park Falls between 30 May and 2 June. Top panel: evolution of XCO_2 (in ppm) from hourly averaged TCCON data (black dots), the free run (blue line and dots) and the analysis (red line and dots). The dots are the values of the model in the observation space. Lower panel: evolution of the mean sea level pressure (in hPa, black line) and the temperature at 500 hPa (in K, magenta line). The vertical dotted lines represent 31 May, at 00:00 UTC at 12:00 UTC, and the 1 June, at 00:00 UTC.
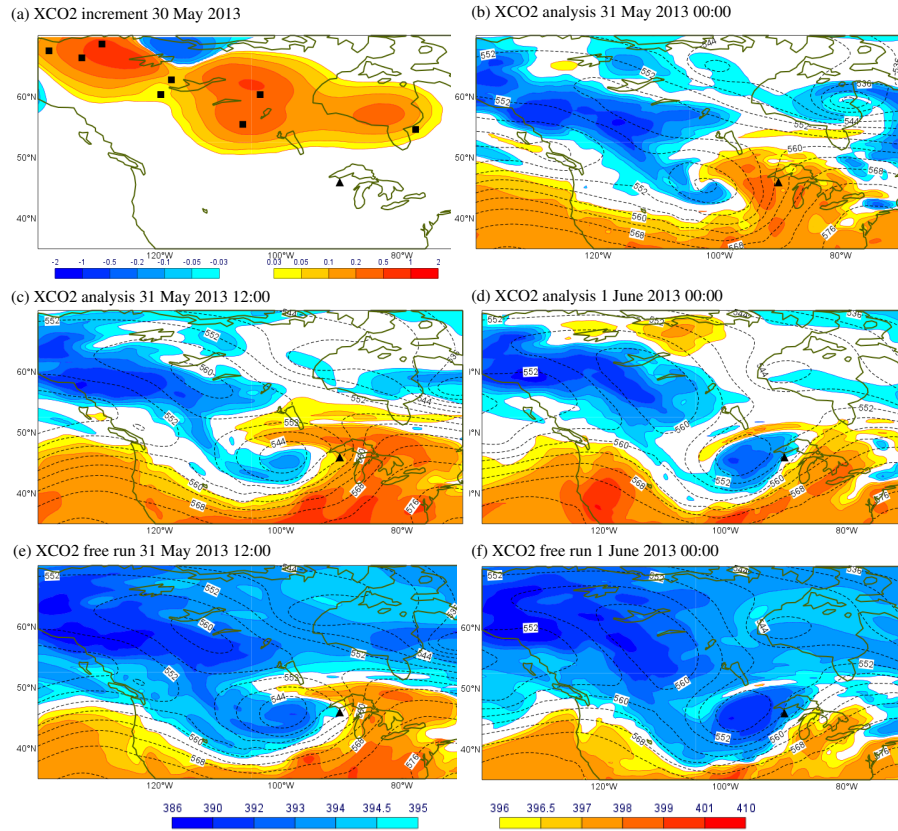
Figure 37. Situation around Park Falls (black triangle), Wisconsin, USA, end of May 2013. **(a)** average increment in terms of XCO$_2$ (in ppm) on 30 May 2013 (contours) and location of the GOSAT measurements during this day (black rectangles). **(b–d)** XCO$_2$ (in ppm) respectively on 31 May at 00:00 UTC, at 12:00 UTC and on 1 June at 00:00 UTC from the analysis. **(e, f)** XCO$_2$ (in ppm) on 31 May at 12:00 UTC and on 1 June at 00:00 UTC from the free run. For **(b)** to **(f)** the dark contours are the values of the geopotential at 500 hPa.
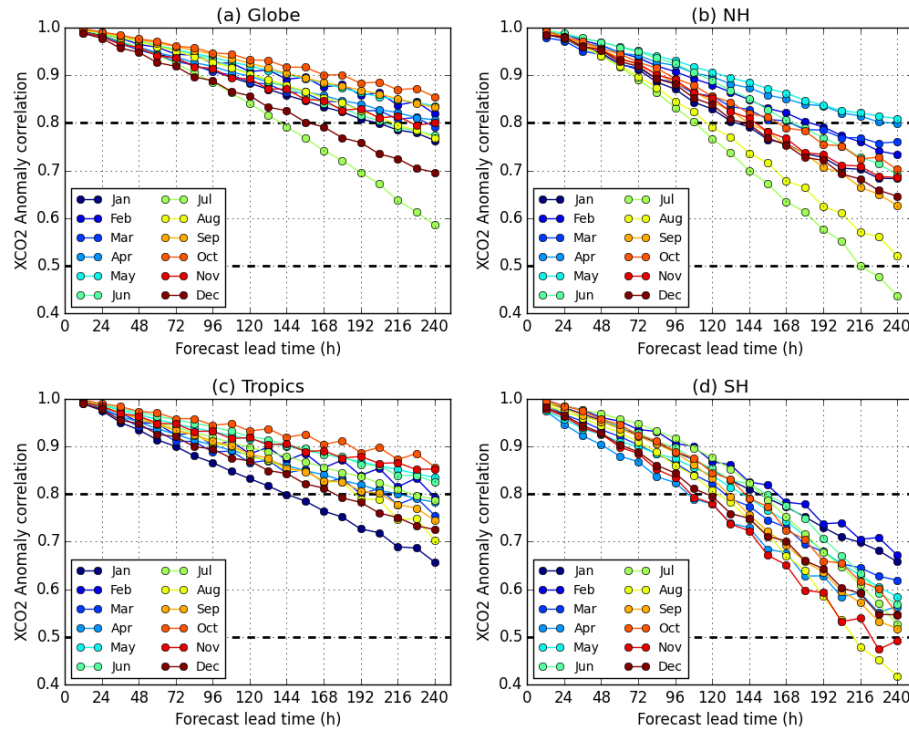
Figure 38. Anomaly correlation coefficient (ACC) of the forecast compared to its own analysis as a function of the forecast lead time and for each month: **(a)** global ACC, **(b)** ACC fot the Northern Hemisphere (20–90° N), **(c)** ACC fot the tropics (20° S–20° N), **(d)** ACC fot the Southern Hemisphere (90–20° S). Each month is represented by a different color (see inset legends).